NIST GCR 12-963

"Layer-by-Layer Assembly of Flame Retardant Coatings for Foam and Fabric." Final Report.

National Institute of Standards and Technology
U.S. Department of Commerce

NIST GCR 12-963

"Layer-by-Layer Assembly of Flame Retardant Coatings for Foam and Fabric." Final Report.

Jamie Grunlan
Department of Mechanical Engineering
3123 Texas A&M University
College Station, TX 77843-3123

Grant #*60NANB8D8104*

February 2012

U.S. Department of Commerce
John E. Bryson, Secretary

National Institute of Standards and Technology
Patrick D. Gallagher, Under Secretary of Commerce for Standards and Technology and Director

Notice

This report was prepared for the Engineering Laboratory of the National Institute of Standards and Technology under Grant number 60NANB8D8104. The statement and conclusions contained in this report are those of the authors and do not necessarily reflect the views of the National Institute of Standards and Technology or the Engineering Laboratory.

"Layer-by-Layer Assembly of Flame Retardant Coatings for Foam and Fabric"
Grant #60NANB8D8104
Period Covered: June 30, 2008 – June 30, 2011

FINAL REPORT

Submitted by Jamie Grunlan
Department of Mechanical Engineering
3123 Texas A&M University
College Station, TX 77843-3123

Abstract

The accomplishments of the project are summarized in three published studies, which follow this abstract and constitute this final report. The studies use layer by layer assembly methods to investigate material flammability.

In the first study, entitled, "Growth and fire resistance of colloidal silica-polyelectrolyte thin film assemblies," thin films of colloidal silica were deposited on cotton fibers via layer-by-layer (LbL) assembly in an effort to reduce the flammability of cotton fabric.

In the second study, entitled, "Growth and fire protection behavior of POSS-based multilayer thin films," fully siliceous layer-by-layer assembled thin films, using polyhedral oligomeric silsesquioxanes (POSS) as building blocks, were successfully deposited on various substrates, including cotton fabric.

In the third study, entitled, "Intumescent All-Polymer Multilayer Nanocoating Capable of Extinguishing Flame on Fabric," LbL assemblies of PSP and PAAm were successfully deposited on various substrates, including cotton fabric.

Keywords:

Calorimetry; flammability; layer by layer assembly; nanoparticles; thin films

Executive Summary

In the first study, entitled, "Growth and fire resistance of colloidal silica-polyelectrolyte thin film assemblies," thin films of colloidal silica were deposited on cotton fibers via layer-by-layer (LbL) assembly in an effort to reduce the flammability of cotton fabric. Negatively charged silica nanoparticles of two different sizes (8 and 27 nm) were paired with either positively charged silica (12 nm) or cationic polyethylenimine (PEI). PEI/silica films were thicker due to better (more uniform) deposition of silica particles that contributed to more than 90% of the film weight. Each coating was evaluated at 10 and 20 bilayers (BL). All coated fabrics retained their weave structure after being exposed to a vertical flame test, while uncoated cotton was completely destroyed. Micro combustion calorimetry confirmed that coated fabrics exhibited a reduced peak heat release rate, by as much as 20% relative to the uncoated control. The 10 BL PEI-8 nm silica recipe was the most effective because the coating is relatively thick and uniform relative to the other systems. Soaking cotton in basic water (pH 10) prior to deposition resulted in better assembly adhesion and flame-retardant behavior. These results demonstrate that LbL assembly is a useful technique for imparting flame retardant properties through conformal coating of complex substrates like cotton fabric.

In the second study, entitled, "Growth and fire protection behavior of POSS-based multilayer thin films," fully siliceous layer-by-layer assembled thin films, using polyhedral oligomeric silsesquioxanes (POSS) as building blocks, were successfully deposited on various substrates, including cotton fabric. Water soluble OctaAmmonium POSS ((+)POSS) and OctaTMA POSS ((-)POSS) were used as cationic and anionic components for thin film deposition from water. Aminopropyl silsesquioxane oligomer (AP) was also used as an alternative cationic species. The thickness of the AP/(-)POSS and (+)POSS/(-)POSS film is shown to increase linearly with bilayers deposited. Thermogravimetric analysis (TGA), vertical flame testing (VFT), microscale combustion calorimetry (MCC) and pill testing were performed on cotton fabric coated with 5–20 bilayers of a given recipe. All coated fabrics showed improved preservation (i.e., greater residue following heating to 600 ^{o}C) and resistance to degradation from direct flame. With less than 8 wt % added to the total fabric weight, more than 12 wt % char remained following MCC for the 20 bilayers (+)POSS/(-)POSS coated cotton. Furthermore, afterglow time was reduced and the fabric weave structure and shape of the individual fibers were highly preserved following VFT. It is expected that this environmentally-friendly coating could be used to impart flame retardant behavior to a variety of fabrics.

In the third study, entitled, "Intumescent All-Polymer Multilayer Nanocoating Capable of Extinguishing Flame on Fabric," LbL assemblies of PSP and PAAm were successfully deposited on various substrates, including cotton fabric. By applying these thin coatings on fabric, afterglow is eliminated and after-flame time is reduced. Flame was completely extinguished on fabric coated with 20 BL of PSP/ PAAm. Post-burn chars were imaged with SEM and the weave structure, and fiber shape and structure, are shown to be well preserved. Especially on the 20 BL char, bubbles were formed on the fiber surfaces during burning, which is believed due to an intumescent effect. From microscale calorimetry data, the peak heat release rate and total heat release of fabric show a 43% and 51% reduction compared to the control fabric, with only 1.7 wt% coating added. This work demonstrates the first ever intumescent nanocoating prepared using LbL assembly. These all-polymer coatings provide an environmentally friendly alternative for protecting fabrics (no need for chemical treatments) such as cotton and lay the groundwork for rendering many other complex substrates (e.g., foam) flame-retardant without altering their processing and desirable mechanical behavior. The opportunity for further improvements is tremendous through the use of alternate polymers, nanoparticles, and/ or smaller molecules that may enhance these effects.

Journal of Colloid and Interface Science 356 (2011) 69–77

Contents lists available at ScienceDirect

Journal of Colloid and Interface Science

www.elsevier.com/locate/jcis

Growth and fire resistance of colloidal silica-polyelectrolyte thin film assemblies

Galina Laufer [a], Federico Carosio [b], Rico Martinez [a], Giovanni Camino [b], Jaime C. Grunlan [a,*]

[a] Department of Mechanical Engineering, Texas A&M University, College Station, TX 77843, United States
[b] Dipartimento di Scienza dei Materiali e Ingegneria Chimica, Politecnico di Torino, Corso Duca degli Abruzzi 24, 10129 Torino, Italy

ARTICLE INFO

Article history:
Received 19 October 2010
Accepted 22 December 2010
Available online 30 December 2010

Keywords:
Layer-by-layer assembly
Colloidal silica
Polyethylenimine
Flame retardant
Cotton fabric

ABSTRACT

Thin films of colloidal silica were deposited on cotton fibers via layer-by-layer (LbL) assembly in an effort to reduce the flammability of cotton fabric. Negatively charged silica nanoparticles of two different sizes (8 and 27 nm) were paired with either positively charged silica (12 nm) or cationic polyethylenimine (PEI). PEI/silica films were thicker due to better (more uniform) deposition of silica particles that contributed to more than 90% of the film weight. Each coating was evaluated at 10 and 20 bilayers (BL). All coated fabrics retained their weave structure after being exposed to a vertical flame test, while uncoated cotton was completely destroyed. Micro combustion calorimetry confirmed that coated fabrics exhibited a reduced peak heat release rate, by as much as 20% relative to the uncoated control. The 10 BL PEI-8 nm silica recipe was the most effective because the coating is relatively thick and uniform relative to the other systems. Soaking cotton in basic water (pH 10) prior to deposition resulted in better assembly adhesion and flame-retardant behavior. These results demonstrate that LbL assembly is a useful technique for imparting flame retardant properties through conformal coating of complex substrates like cotton fabric.

1. Introduction

Cotton is an incredibly versatile material that is soft, easy to care for, and durable, but it is also highly flammable. With more than 80% of all fire deaths and injuries to civilians due to household fires, and the popularity of cotton fabric in apparel and home furnishings, this flammability presents a significant safety concern [1]. As a result, there are strict safety guidelines for applications such as children's sleepwear and mattresses (16 CFR 1615-6, 16 CFR 1632) [2]. These restrictions limit cotton's appeal and use in these products and place it at a disadvantage compared to other fabrics that contain a high percentage of synthetic fibers with lower flammability. Improved flame resistance is needed to allow cotton to be more widely utilized.

Numerous studies have focused on enhancing the flame-retardant behavior of cotton using chemical modification. By changing the nature of burning from flash to steady, charring, or glowing, these flame resistant additives can slow burning and improve safety [3]. Since the 1980s, some of the commonly used treatments (e.g., brominated compounds) have raised concerns with regard to toxicity and environmental persistence [4,5]. Thin assemblies of polymer and clay, deposited onto cotton fibers using layer-by-layer (LbL) assembly, were recently reported as a more environmentally-friendly flame retardant treatment [6]. LbL deposition consists of building multilayered thin films by consecutive adsorption of oppositely charged polyelectrolytes and/or nanoparticles onto a substrate [7–9]. Each positive and negative pair is referred to as a bilayer (BL). These layers are typically applied to the substrate by dipping or spraying [10–12]. The thickness of each BL is typically 1–100 nm and can be controlled at the nanoscale by altering pH [13,14], molecular weight of the components [15], ionic strength [16], and temperature [14,17]. This versatile process has been used to grow films with antireflective [18–20], oxygen barrier [21], sensing [22–24], electrochromic [25–27], antimicrobial [28–30], and drug delivery [31,32] properties. It has even been used to put layers of poly(sodium 4-styrene sulfonate) (PSS) and poly(allylamine hydrochloride) (PAH) on cotton fibers for potential application in functional textiles [33].

Layered silicates have been investigated extensively as an environmentally friendly alternative to the use of halogenated compounds in flame retardant applications [34–36]. Combining smectite clays with polyelectrolytes in thin films on cotton reduces burn time, afterglow and peak heat release rate [6]. Colloidal silica is another inorganic additive known to reduce flammability [37–39] and has been successfully incorporated into the LbL process [40–42]. The proposed mechanism for this flame-retardant behavior is aggregation of particles on the surface of nanocomposites that forms an insulating layer, which limits heat transfer [43]. Despite improving thermal stability, adding nanoparticles is known to increase viscosity and modify mechanical properties of the final polymeric material, making their use prohibitive for many

* Corresponding author. Fax: +1 979 862 3989.
E-mail address: jgrunlan@tamu.edu (J.C. Grunlan).

0021-9797/$ - see front matter © 2010 Elsevier Inc. All rights reserved.
doi:10.1016/j.jcis.2010.12.072

practical applications [38,44]. With LbL assembly, nanoparticles are deposited directly onto the surface of the substrate as a thin layer, which allows the mechanism of protection to remain without the challenges associated with processing or adversely modifying mechanical behavior.

In the present study, the flammability of cotton fabric is shown to be reduced by depositing bilayers of polyethylenimine and colloidal silica (or positive and negative silica only) via LbL assembly. Growth trends and surface structure of films with varying composition revealed that when PEI is present as the cationic component, thicker and heavier coatings are produced due to better deposition of silica nanoparticles. All systems grow linearly as a function of bilayers deposited, with PEI and 27 nm silica exceeding 200 nm after 20 bilayers of deposition. Ten and 20 BL coatings were evaluated with respect to microstructure and flammability. Microscopic images revealed that 20 BL films were cracking and flaking in all of the systems. As a result, fabrics coated with 10 BL exhibited better flame-retardant behavior (i.e., reduced heat release rate and increased post-burn char). Heat release rate was reduced by all coated samples, but a 10 BL coating of PEI–Ludox SM reduced peak heat release by 20% and heat release rate by 17%. Pre-soaking the cotton in an aqueous NaOH solution before LbL deposition further improves this behavior due to increased negative charge on the surface of the cellulosic fibers [45]. This work demonstrates a simple method for uniformly depositing thin films on the complex surface of cotton fibers and the efficacy of colloidal silica as an alternative to inorganic clay platelets for flame retardant fabric.

Table 1
Properties of colloidal silica dispersions.

	Ludox SM	Ludox TM	Ludox CL
Particle size (nm)	8 ± 3	27 ± 5	12 ± 2
Particle surface charge	Negative	Negative	Positive
Counterion	Na^+	Na^+	Cl^-
Chloride content (wt.%)	–	–	0.03
Sodium content (wt.%)	0.56	0.21	–

2. Materials and methods

2.1. Material

Anionic deposition solutions consisted of 1.0 wt.% colloidal silica, with particle diameters of 27 ± 5 or 8 ± 3 nm (tradename Ludox TM and Ludox SM, respectively) (Aldrich, Milwaukee, WI), in deionized water (18.2 MΩ). Cationic solutions were prepared by adding 0.1 wt.% of branched polyethylenimine (PEI), with molecular weight of 25,000 g/mol (Aldrich, Milwaukee, WI), or 1 wt.% of CS with 12 ± 2 nm diameter (tradename Ludox CL) (Aldrich, Milwaukee, WI) to deionized water. Specifications of Ludox particles are summarized in Table 1. The pH of the PEI was adjusted to 10 with hydrochloric acid (HCl). Single-side-polished (1 0 0) silicon wafers (University Wafer, South Boston, MA) were used as a substrate for film thickness characterization. For the pre-soaking solution, sodium hydroxide (NaOH) was added to deionized water until pH 10 was achieved. Cotton fabric was supplied by the USDA Southern Regional Research Center (New Orleans, LA). The fabric was a balanced weave with approximately 80 threads per inch in both the warp and fill direction, with a weight of 119 g/m^2.

2.2. Film deposition

Prior to deposition, the silicon wafers were rinsed with acetone and deionized water, and then dried with filtered air. In the case of cotton, it was dried in the oven for 1 h at 70 °C prior to deposition. All films were deposited on a given substrate (Si wafer or cotton fabric) using the procedure shown schematically in Fig. 1. The substrates were alternately dipped into positive and negative mixtures. Initial dips were 5 min and each subsequent dip was 1 min. Each dip was followed by rinsing with deionized water and, in case of silicon wafer, drying with air. For NaOH treated cotton, it was soaked in a pH 10 solution for 1 min prior LbL deposition. Fabrics were wringed out to expel liquid as an alternative to the traditional drying step. After the desired number of bilayers was achieved, fabrics were dried at 70 °C in an oven for 2 h before testing.

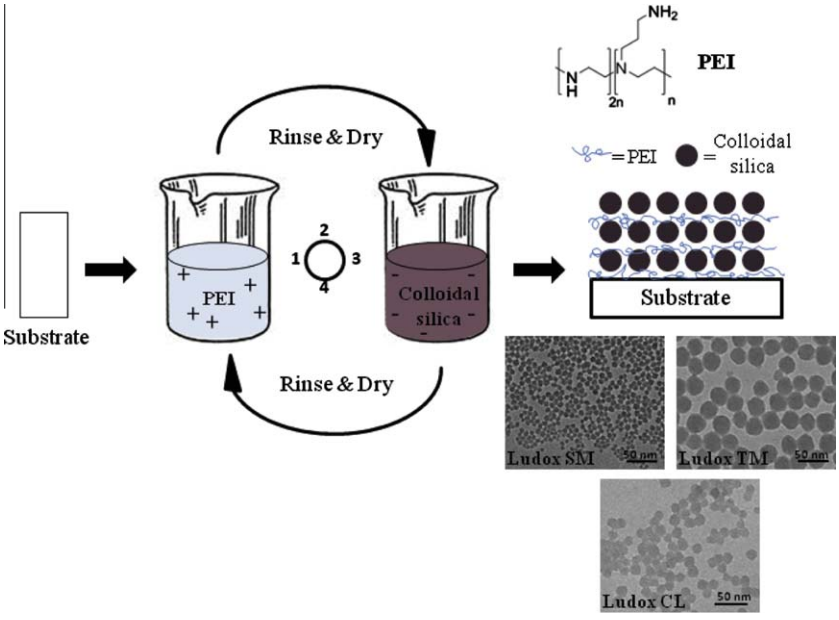

Fig. 1. Schematic representation of layer-by-layer assembly. Steps 1–4 are repeated until the desired number of bilayers is achieved.

2.3. Film characterization

Film thickness was measured with a PHE-101 Discrete Wavelengh Ellipsometer (Microphotonics, Allentown, PA). The 632.8 nm laser was used at an incidence angle of 65°. The weight per deposited layer was measured with a Maxtek Research Quartz Crystal Microbalance (RQCM) (Infinicon, East Syracuse, NY), with a frequency range of 3.8–6 MHz, in conjunction with 5 MHz quartz crystals. Cross sections of the films were imaged with a JEOL 1200 EX transmission electron microscope (Mitaka, Tokyo, Japan), operated at 110 kV. Samples were prepared for imaging by embedding a piece of fabric supporting the LbL film in epoxy and sectioning it with a microtome equipped with a diamond knife. Surface images of control and coated fabrics before and after the flame test were acquired with a Quanta 600 FE-SEM (FEI Company, Hillsboro, OR).

2.4. Flame retardant characterization

All tests were conducted in triplicate for each of the systems examined. The thermal stability of uncoated and coated fabrics was measured with a Q50 Thermogravimetric Analyzer (TA Instruments, New Castle, DE). Each sample weighed approximately 20 mg and was run under air from room temperature to 600 °C, at a heating rate of 20 °C/min. Vertical flame tests were conducted on coated and virgin fabrics according to ASTM D6413-08 using an Automatic Vertical Flammability Cabinet, model VC-2 (Govmark, Farmingdale, NY). Micro combustion calorimeter, model MCC-1 (Govmark), tests were performed at the University of Dayton Research Institute (Dayton, OH). Samples were tested at a 1 °C/s heating rate under nitrogen from 200 to 600 °C using method A of ASTM D7309, without additional conditioning prior to testing.

3. Results and discussion

3.1. Film growth and microstructure

The growth of four different colloidal silica-based assemblies (PEI–Ludox SM, PEI–Ludox TM, Ludox CL–Ludox SM, and Ludox CL–Ludox TM) was monitored with ellipsometry, as shown in Fig. 2a. All four systems grow linearly as a function of bilayers deposited. When polyethylenimine is one of the two components, the films grow at a much higher rate as compared to all-silica films. It is possible that PEI provides better adsorption conditions for silica particles due to its flatter (or smoother) deposition and low

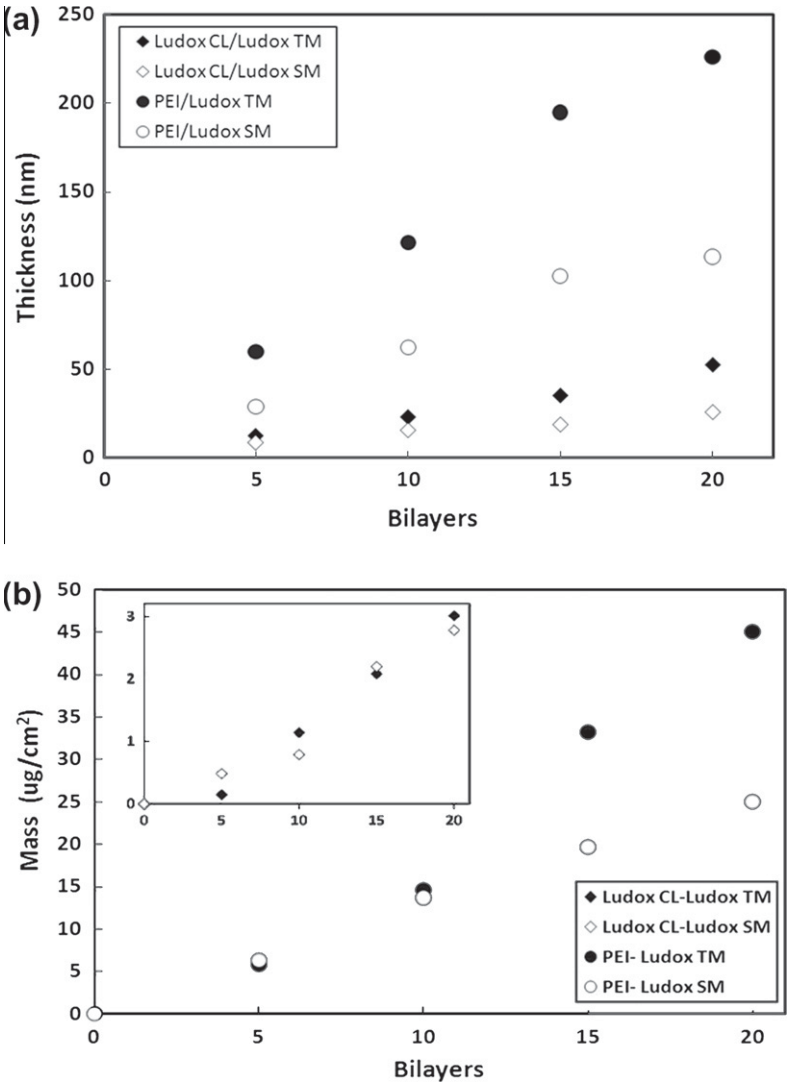

Fig. 2. Thickness (a) and mass (b) of four different silica-based LbL assembly compositions as function of bilayers deposited. The inset of (b) shows the much lighter (thinner) growth of the all-silica systems.

modulus. PEI is commonly used as a primer layer for LbL deposition due to its adhesive characteristics [46–48]. In all cases, with or without PEI, the average thickness of a bilayer is significantly smaller than a single silica particle diameter. It has been reported that at the initial stages of growth, nanoparticles form isolated domains, which lead to incomplete surface coverage [49]. This effect may be exaggerated for all-silica assemblies due to relatively weak adhesion between layers. A combination of this inhomogeneous film growth and seating of colloidal particles in the interstitial spaces of the preceding layer is believed to account for this thin growth.

To further investigate film growth, a quartz crystal micro balance was used to measure mass increase per layer deposited, as shown in Fig. 2b. The growth behavior of all systems is similar to the linear trend observed with ellipsometry, with the growth rate of PEI–silica being larger than that of silica–silica. The weight of a 5 BL PEI–silica system is more than a 20 BL all-silica film. From Table 2, it can be seen that silica is the main ingredient contributing to weight, with PEI being less than 10 wt.% in the film. Not only is silica a higher density material, its thickness per layer is much greater. It has already been observed that PEI only deposits ~3.5 nm per layer at pH 10 [21]. Table 2 also shows that films with smaller silica particles (Ludox SM) always result in higher density. A tighter packing of particles around the cotton fiber should reduce the surface of the fiber exposed to flame. As expected, coatings made with this smaller silica, exhibit better flame retardant properties than coatings made with the larger Ludox TM (see Tables 3 and 4).

3.2. Deposition on cotton fabric

Fig. 3 shows cross sections of single cotton fibers coated with 20 BL of Ludox CL–Ludox TM (Fig. 3a) and 20 BL of PEI–Ludox TM (Fig. 3b). These systems are highlighted because the relatively large particle diameters are easier to visualize. Lack of coating thickness uniformity observed in these images is likely the result of fibers touching one another during LbL deposition and loss of coating during sectioning due to the weakly charged cellulose surface, which causes the assemblies to attach to the surface more weakly than to more highly charged, smooth surfaces (e.g., Si wafer). Additionally, the difference in modulus between the cellulosic substrate and silica-based coatings may contribute to some cracking and flaking. Since coating deposited on fiber's surface is less than 250 nm thick, it does not modify the esthetics and feel of the fabric.

Fig. 4 shows the difference in fiber coverage between 10 and 20 BL coatings. Fibers coated with 10 BL of Ludox CL–Ludox TM (Fig. 4a) are fully covered, but uncoated spots are observed on the fiber's surface with 20 BL (Fig. 4b). A similar trend is observed with the PEI–Ludox TM system, where the 10 BL coating (Fig. 4c) looks heavier than the 20 BL coated fibers (Fig. 4d). This suggests that a 20 BL coating is too heavy to be held by weak charges on the cotton fiber's surface. It is expected that fabric coated with 10 BL will exhibit better flame retardant properties due to this more complete coverage of the fibers. It should also be noted that PEI-containing coatings (Fig. 4c and d) appear much thicker than all-silica coatings (Fig. 4a and b). This observation supports the ellipsometric thicknesses data (Fig. 2a) and suggests the PEI-based coatings will exhibit better anti-flammable behavior.

As discussed above, cotton's low surface charge is one of the contributing factors to flaking of the coating. Untreated cotton has non-cellulose compounds such as waxes, pectins, and proteins on its outer surface which diminish surface charge [50]. This surface charge can be increased, and the contaminants removed, by exposing the cotton fabric to an aqueous NaOH solution at pH 10 [45]. At pH 10 this solution is relatively dilute, so there is no damage to the fibers. This NaOH treatment allows the initial layers to better anchor themselves to the fabric and provide improved adhesion for subsequent layer deposition. Fig. 5 shows the difference in fiber coverage for untreated and NaOH pretreated 10 BL PEI–Ludox SM (Fig. 5b). The treated fabric clearly exhibits a heavier and more evenly distributed coating (and higher weight gain for 10 BL in Table 3), which ultimately provides greater residue in the TGA (see Table 3).

3.3. Flame resistance and thermal stability of fabric

Cotton fabric was coated with 10 and 20 bilayers of the four systems described in the previous section. The weight added to fabrics was determined by weighing before and after coating (reported as percent of original mass in Table 3). Fabric weight gain does not show the same trend observed with QCM, where films with Ludox TM had a higher weight gain. This observation can be explained by the different chemistries of the deposition substrates. As mentioned earlier, the surface charge of cotton fabric is weak and the coating partially flakes off as it reaches a critical thickness (or mass) that cannot be supported by the weak charge. Films with Ludox TM (27 nm diameter) grow thicker and heavier, so they will experience flaking of the coating earlier than those with Ludox SM (8 nm diameter).

Fig. 6 shows TGA results for the four different coating systems at 10 (Fig. 6a) and 20 BL (Fig. 6b). Coated fabrics show a slightly slower degradation from 100 to 300 °C and a significantly higher residue as compared to the control at final stage of the test. As

Table 2
Composition and density of colloidal silica assemblies.

	Cation (wt.%)	Anion (wt.%)	Density (g/cm^3)
Ludox CL/Ludox SM	75	25	1.36
Ludox CL/Ludox TM	58	42	1.06
PEI/Ludox SM	7.9	92.1	1.72
PEI/Ludox TM	8.1	91.9	1.45

Table 3
Coating weight added to fabrics and residue after heat treatment.

	# BL	% Gain	% Residue (@ 500 °C)	% Residue (@ 600 °C)
Control			5.3	0.2
Ludox CL/Ludox SM	10	3.49	10.7	3.9
	20	5.79	10.7	4.6
Ludox CL/Ludox TM	10	1.98	8.8	2.7
	20	2.01	6.9	1.8
PEI/Ludox SM	10	5.65	13.6	4.7
	10^{NaOH}	6.88	15.7	5.9
	20	8.13	14	6.0
PEI/Ludox TM	10	4.96	11.8	4.3
	20	5.07	11.8	4.5

Table 4
Micro combustion calorimeter results for various coatings on cotton fabrics.

	BL	Char yield (wt.%)	pkHRR (W/g)	pkHRR (°C)	Total HR (kJ/g)
Control	–	4.98	285	381	12.8
Ludox CL/Ludox SM	10	9.53	253	375	11.7
	20	9.58	243	365	11.7
Ludox CL/Ludox TM	10	6.89	240	361	12.2
	20	6.27	245	361	12.4
PEI/Ludox SM	10	13.07	227	390	10.5
	20	13.02	234	388	11.2
PEI/Ludox TM	10	9.59	258	386	11.6
	20	9.04	268	380	11.5

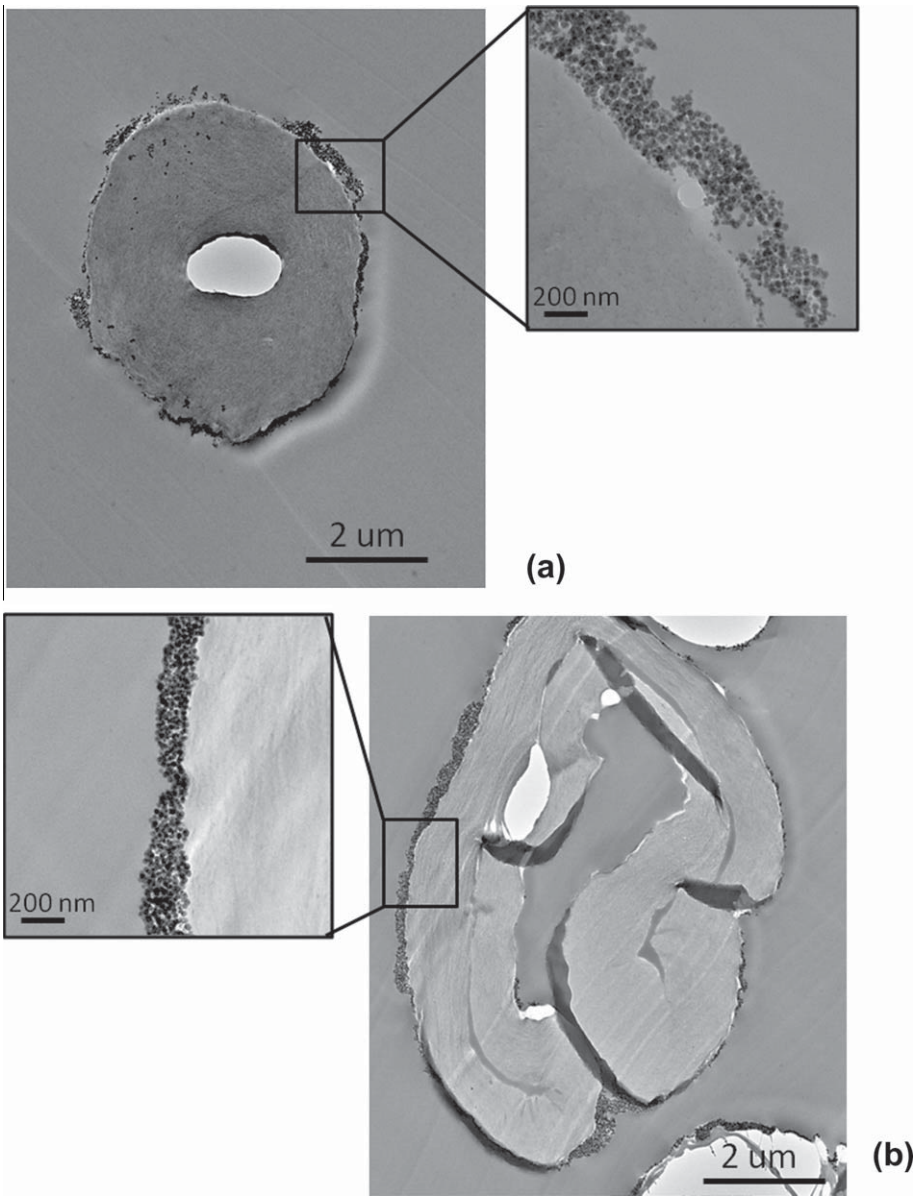

Fig. 3. TEM cross section of cotton fiber with 20 BL Ludox CL–Ludox TM (a) and 20 BL PEI–Ludox TM (b) coatings.

expected, systems containing Ludox SM perform better than systems with Ludox TM. Also worth noting is that samples coated with 10 BL produced the same or greater residue than fabrics coated with 20 BL of the identical composition. The residue amounts for the control fabric and each coated fabric are summarized in Table 3. For the most part, the weight retained after heating to 600 °C is proportional to the initial coating weight. The amounts of char obtained after heating correlate well with flame retardance [51]. In all cases, the coated fabric had at least an order of magnitude greater residue than the control.

Vertical flame testing (ASTM D6413) was used to evaluate the coated fabric's flammability. After ignition, flame spreads slower on coated fabrics and, as a result, these fabrics also have twice the afterflame time (fire on the sample after direct flame is removed) compared to the control. Despite the longer afterflame, afterglow was reduced by at least 17 s for coated fabrics. Afterglow time is important because it shows how long fabric continues to burn without flame and longer afterglow increases the chances of fire reigniting. Following the test, there was no fabric left on the control sample holder, as shown in Fig. 7. Coatings with Ludox CL–Ludox SM and PEI–Ludox SM (i.e., smaller silica) left the highest amounts of residue. As discussed earlier, tightly packed silica particles shield cotton fibers from rapid degradation at high temperatures by reducing cotton availability on the surface. Samples coated with Ludox CL–Ludox TM and PEI–Ludox TM (i.e., larger silica) did not perform as well due to lower packing density, but still retained a significant amount of residue.

Following burning, the surfaces of all fabrics were imaged with SEM to evaluate the retention of fabric structure. The after burn image of the uncoated control is omitted because there was no fabric left after the vertical flame test. All four coated samples were able to preserve the fabric weave structure, although significant shrinking of individual fibers is observed in Fig. 8 (for most systems). Fiber shrinkage is somewhat expected due to poor packing of spherical nanoparticles and non-inform coverage of fibers that cannot provide as effective of a protective shell for cotton, which contributes to the further degradation of fibers, especially for larger silica coatings (Fig. 8d and e). Higher magnification of

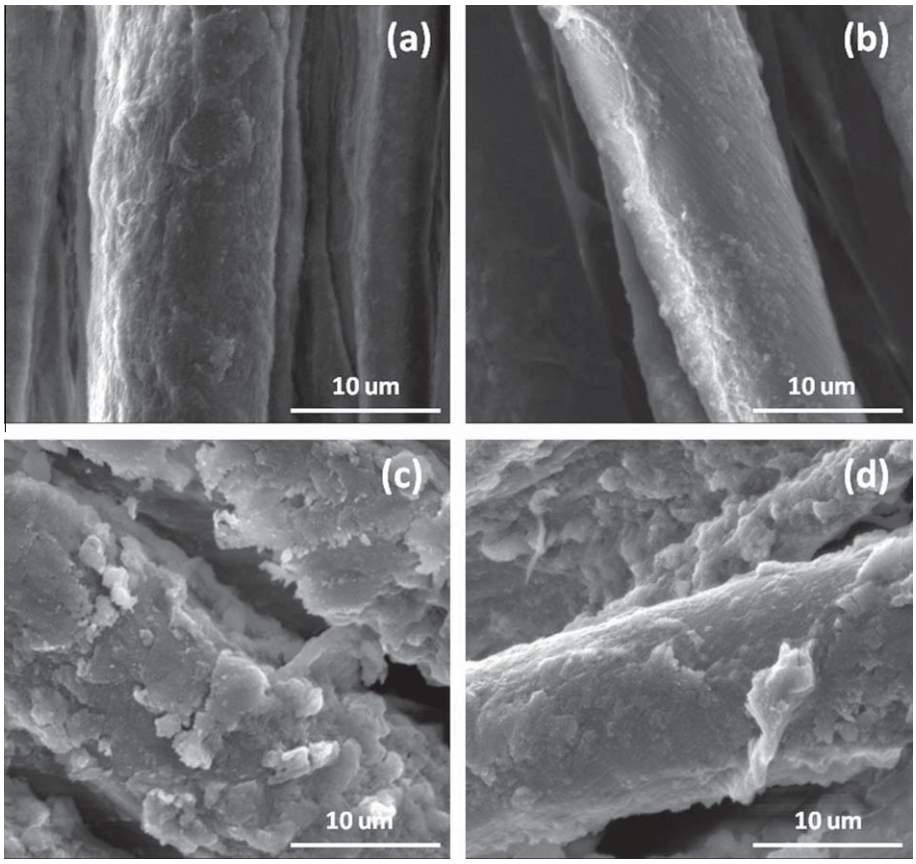

Fig. 4. SEM images of cotton fabric coated with 10 BL (a) and 20 BL (b) Ludox CL–Ludox TM, and10 BL (c) and 20 BL (d) PEI–Ludox TM.

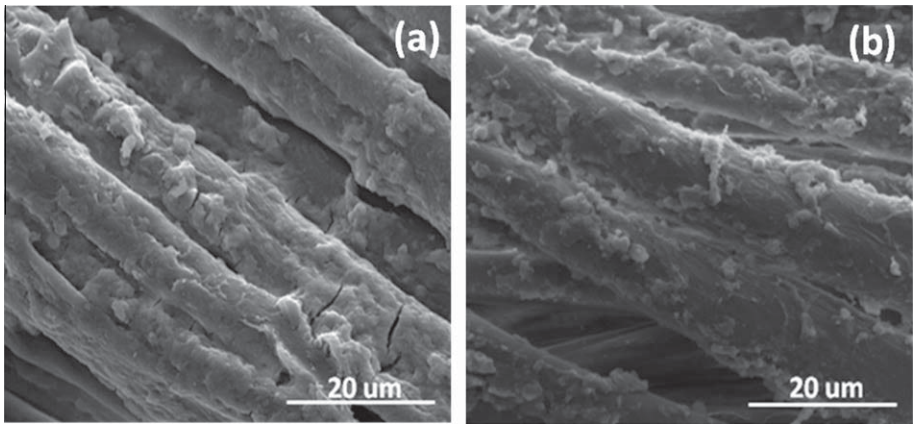

Fig. 5. SEM of cotton fibers coated with 10 BL PEI–Ludox SM with (a) and without (b) NaOH pretreatment.

Fig. 8e confirms cracking of the coating, which is likely due to the high modulus and weaker bonding of this larger silica system (Ludox CL–Ludox TM). The highest magnification image, with 1 μm scale bar, clearly shows the colloidal nature of the coating and its protective shell nature.

Micro combustion calorimetry (MCC) was used to evaluate heat release during burning of these cotton fabrics. MCC is a small scale instrument that measures the heat of combustion of the pyrolysis products by oxygen consumption calorimetry. Fabrics were tested under nitrogen up to 600 °C. These heat release measurements are summarized in Table 4. Peak heat release rate (pkHRR) is the maximum heat release rate during the experiment. The higher the pkHRR value, the more heat is given off by the sample. The temperature at which pkHRR occured and the total heat release (HR) are shown in Table 4. All coated fabrics show a higher residue mass and a decreased pkHRR, as compared to the control. Comparison of HRR curves between control and fabrics coated with 10 BL PEI/Ludox SM and Ludox CL/Ludox SM is shown in Fig. 9. Both coatings are clearly shown to reduce the peak heat release rate, although onset of heat release occurs at a 10–20 °C lower temperature. This modest reduction in onset may be due to the porous nature of the fully colloidal coating, which would be expected to have significantly enhanced surface area and gas permeability relative to the PEI/Ludox SM system. The maximum reduction in pkHRR (20 %) and HRR (17%) was observed in the fabric coated with 10 BL of PEI/Ludox SM, which agrees well with TGA results.

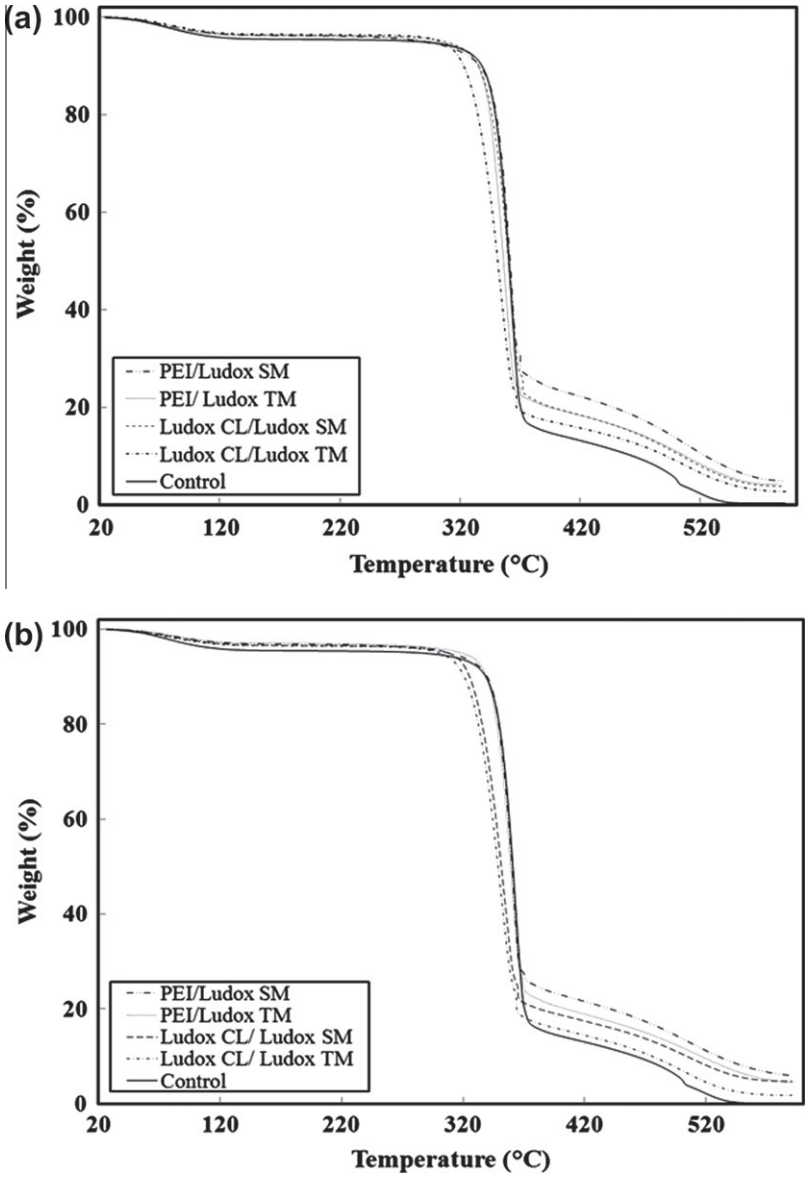

Fig. 6. Weight loss as a function of temperature for uncoated (control) and 10 BL (a) or 20 BL (b) coated fabrics.

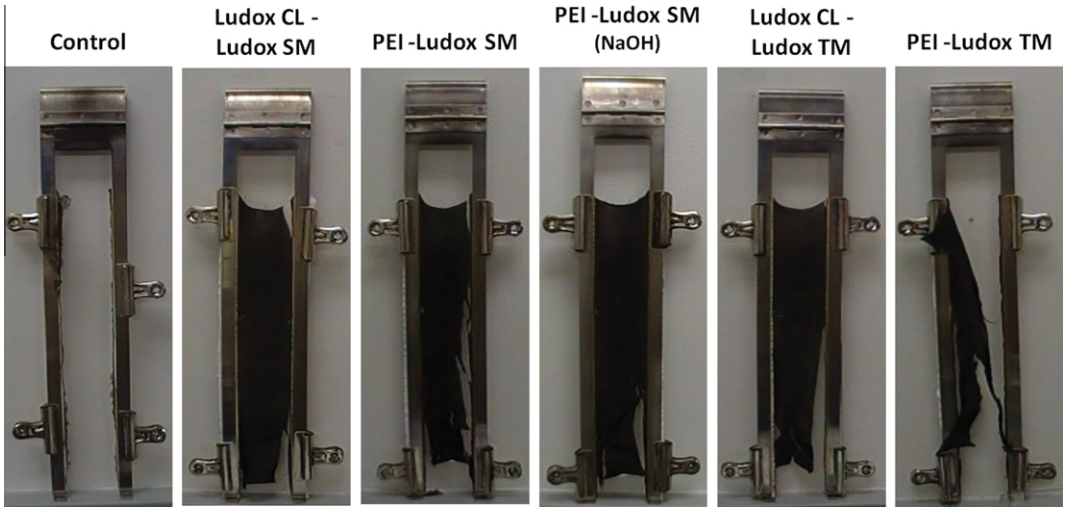

Fig. 7. Images of control and 10 BL coated fabrics following vertical burn testing.

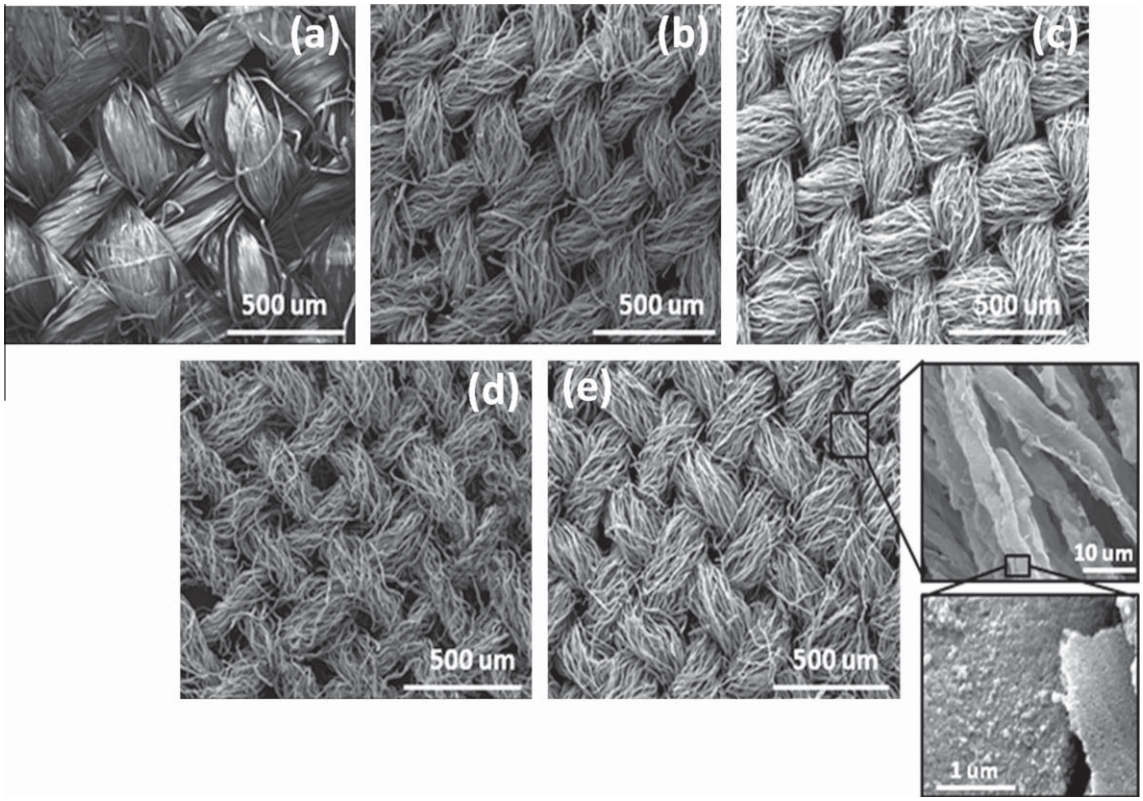

Fig. 8. SEM images of control fabric before vertical flame test (a), and 10 BL coated fabrics following the vertical burn test: PEI–Ludox SM (b), Ludox CL–Ludox SM (c), PEI–Ludox TM (d), and Ludox CL–Ludox TM (e).

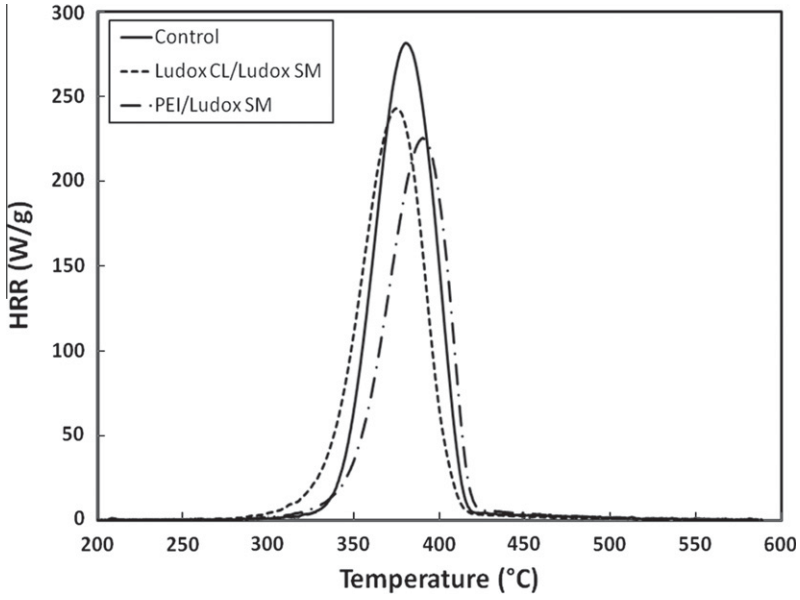

Fig. 9. Heat release rate as a function of temperature, measured with micro combustion calorimetry, for uncoated cotton and 10 BL coated fabric. Testing was performed by heating at 1 °C/s under N_2.

This same coating also produced the greatest amount of char (~13 wt.%), which is more than double the coating weight (see Table 3). Increasing the number of bilayers to 20 does not improve thermal stability of the fabrics based on the MCC data. This was expected based upon the patchy appearance of the coating due to cracking and flaking (see Fig. 4).

4. Conclusions

Silica-based thin film assemblies were deposited on cotton fabric to impart flame-retardant behavior. All assemblies exhibited linear growth as a function of the number of bilayers deposited. The presence of PEI as the cationic component resulted in

significantly thicker and heavier coatings. When cotton was used as a deposition substrate, coatings containing larger silica (i.e., Ludox TM with 27 nm particle diameter) appear to flake off at 20 BL due to weak fabric surface charge and high coating mass. Treating cotton fabric with an aqueous NaOH solution prior to LbL assembly increases negative charge of the substrate and results in improved deposition and flame-retardant behavior compared to coating on untreated cotton. The flame retardant properties of 10 and 20 BL coated fabric were tested using TGA, vertical flame, and micro combustion calorimetry. All of the coated fabrics left a significant amount of char following the vertical flame test and retained the fabric weave structure, as observed by SEM. Additionally, micro calorimeter testing revealed a lower peak heat release rate for coated fabrics. With respect to silica particle size, coatings made with small silica particles (~8 nm) resulted in better flame retardant properties relative to those made with large particles (~27 nm). Smaller colloids achieve a higher practical packing density around the cotton fibers. This work demonstrates a simple and convenient method for depositing flame retardant thin films on cotton, a very complex substrate geometry, using relatively benign ingredients (from an environmental standpoint). More work is underway to reduce cotton flammability with other nanoparticles (e.g., layered hydroxides) and surface treatments.

Acknowledgments

The NIST Building and Fire Research Lab, Huntsman Corporation, and Texas Engineering Experiment Station (TEES) are acknowledged for financial support of this work. The authors also thank Z. Levin, M. Priolo, and Y.T. Park for assistance with SEM (Levin) and TEM (Priolo and Park) images. The FE-SEM acquisition was supported in part by the National Science Foundation under Grant No. DBI-0116835.

References

[1] US Fire Administration, National Fire Protection Association Fire Loss, 2008.
[2] S. Gallagher, J. Campbell, Siloxane–Phosphonate Finishes on Cellulose: Thermal Characterization and Flammability Data, Beltwide Cotton Conference, San Antonio, TX, 2004, pp. 2443–2847.
[3] S.G. Horvat, J. Coated Fabrics 22 (1992) 161–171.
[4] C.A. de Wit, Chemosphere 46 (2002) 583–624.
[5] I. Watanabe, S. Sakai, Environ. Int. 29 (2003) 665–682.
[6] Y.C. Li, J. Schulz, S. Mannen, C. Delhom, B. Condon, S. Chang, M. Zammarano, J.C. Grunlan, ACS Nano 4 (2010) 3325–3337.
[7] G. Decher, M. Eckle, J. Schmitt, B. Struth, Curr. Opin. Colloid Interface Sci 3 (1998) 32–39.
[8] G. Decher, F. Essler, J.D. Hong, K. Lowack, J. Schmitt, Y. Lvov, Abstracts Papers Am. Chem. Soc. 205 (1993) 334–POLY.
[9] P. Hammond, Adv. Mater. 16 (2004) 1271–1293.
[10] W.-S. Jang, J.C. Grunlan, Rev. Sci. Instrum. 76 (2005) 1–4.
[11] J.B. Schlenoff, S.T. Dubas, T. Farhat, Langmuir 16 (2000) 9968–9969.
[12] A. Izquierdo, S.S. Ono, J.-C. Voegel, P. Schaaf, G. Decher, Langmuir 21 (2005) 7558–7567.
[13] S.S. Shiratori, M.F. Rubner, Macromolecules 33 (2000) 4213–4219.
[14] L. Chang, X. Kong, F. Wang, L. Wang, J. Shen, Thin Solid Films 516 (2008) 2125–2129.
[15] Z. Sui, D. Salloum, J.B. Schlenoff, Langmuir 19 (2003) 2491–2495.
[16] R.A. McAloney, M. Sinyor, V. Dudnik, M.C. Goh, Langmuir 17 (2001) 6655–6663.
[17] H.L. Tan, M.J. McMurdo, G.Q. Pan, P.G. Van Patten, Langmuir 19 (2003) 9311–9314.
[18] J. Hiller, J.D. Mendelsohn, M.F. Rubner, Nat. Mater. 1 (2002) 59–63.
[19] J. Cho, J. Hong, K. Char, F. Caruso, J. Am. Chem. Soc. 128 (2006) 9935–9942.
[20] X. Zhang, A. Fujishima, M. Jin, A.V. Emeline, T. Murakami, J. Phys. Chem. 110 (2006) 25142–25148.
[21] M.A. Priolo, D. Gamboa, J.C. Grunlan, ACS Appl. Mater. Interfaces 2 (2010) 312–320.
[22] L. Shen, N. Hu, Biomacromolecules 6 (2005) 1475–1483.
[23] X.B. Yan, X.J. Chen, B.K. Tay, K.A. Khor, Electochem. Commun. 9 (2007) 1269–1275.
[24] P.H. Aoki, D. Volpati, A. Riul, W. Caetano, C.J.L. Constantino, Langmuir 25 (2009) 2231–2338.
[25] Y.T. Park, J.C. Grunlan, Electrochim. Acta 55 (2010) 3257–3267.
[26] D.M. DeLongchamp, M. Kastantin, P.T. Hammond, Chem. Mater. 15 (2003) 1575–1586.
[27] S. Liu, D.G. Kurth, H. Mohwald, D. Volkmer, Adv. Mater. 14 (2002) 225–228.
[28] C.M. Dvoracek, G. Sukhonosova, M.J. Benedik, J.C. Grunlan, Langmuir 25 (2009) 10322–10328.
[29] P. Podsiadlo, S. Paternel, J.-M. Rouillard, Z. Zhang, J. Lee, J.W. Lee, E. Gulari, N.A. Kotov, Langmuir 21 (2005) 11915–11921.
[30] Z. Li, D. Lee, X. Sheng, R.E. Cohen, M.F. Rubner, Langmuir 22 (2006) 9820–9823.
[31] M. Macdonald, N.M. Rodriguez, R. Smith, P.T. Hammond, J. Controlled Release 131 (2008) 228–234.
[32] F. Caruso, D. Trau, H. Mohwald, R. Renneberg, Langmuir 16 (2000) 1485–1488.
[33] K. Hyde, M. Rusa, J. Hinestroza, Nanotechnology 16 (2005) S422–S428.
[34] G. Guo, C.B. Park, Y.H. Lee, Y.S. Kim, M. Sain, Polym. Eng. Sci. 47 (2007) 330–336.
[35] M. Si, M. Goldman, G. Rudomen, M.Y. Gelfer, J.C. Sokolov, M.H. Rafailovich, Macromol. Mater. Eng. 291 (2006) 602–611.
[36] L. Song, Y. Hu, Y. Tang, R. Zhang, Z. Chen, W. Fan, Polym. Degrad. Stab. 87 (2005) 111–116.
[37] S. Hribernik, M.S. Smole, K.S. Kleinschek, M. Bele, J. Jamnik, M. Gaberscek, Polym. Degrad. Stab. 92 (2007) 1957–1965.
[38] T. Kashiwagi, J.W. Gilman, K.M. Butler, R.H. Harris, J.R. Shields, Fire Mater. 24 (2000) 277–289.
[39] F. Yang, G.L. Nelson, J. Appl. Polym. Sci. 91 (2004) 3844–3850.
[40] Z. Lu, S. Eadula, Z. Zheng, K. Xu, G. Grozdits, Y. Lvov, Colloids Surf., A 292 (2007) 56–62.
[41] Y. Lvov, K. Ariga, M. Onda, O. Mitsuhiko, I. Ichinose, T. Kunitake, Langmuir 13 (1997) 6195–6203.
[42] D. Lee, Z. Gemici, M.F. Rubner, R.E. Cohen, Langmuir 23 (2007) 8833–8837.
[43] T. Kashiwagi, A.B. Morgan, J.M. Antonucci, M.R. VanLandingham, J. Harris, J.R. Shields, J. Appl. Polym. Sci. 89 (2003) 2072–2078.
[44] F. Yang, G.L. Nelson, Polym. Adv. Technol. 17 (2006) 320–326.
[45] V. Ribitsch, K. Stana-Kleinschek, S. Jeler, Colloid Polym. Sci. 274 (1996) 388–394.
[46] R. Ma, T. Sasaki, Y. Bando, J. Am. Chem. Soc. 126 (2004) 10382–10388.
[47] A. Reisch, J.-C. Voegel, E. Gonthier, G. Decher, B. Senger, P. Schaaf, P.J. Mesini, Langmuir 25 (2009) 3610–3617.
[48] R. Pei, X. Cui, X. Yang, E. Wang, Biomacromolecules 2 (2001) 463–468.
[49] J.W. Ostrander, A.A. Mamedov, N.A. Kotov, J. Am. Chem. Soc. 123 (2001) 1101–1110.
[50] J. Buchert, J. Pere, L.S. Johansson, J.M. Campbell, Text. Res. J. 71 (2001) 626–629.
[51] S. Nakanishi, T. Hashimoto, Text. Res. J 68 (1998) 807–813.

Journal of Materials Chemistry

Cite this: *J. Mater. Chem.*, 2011, **21**, 3060

www.rsc.org/materials

PAPER

Growth and fire protection behavior of POSS-based multilayer thin films

Yu-Chin Li, Sarah Mannen, Jessica Schulz and Jaime C. Grunlan*

Received 2nd November 2010, Accepted 21st December 2010
DOI: 10.1039/c0jm03752d

Fully siliceous layer-by-layer assembled thin films, using polyhedral oligomeric silsesquioxanes (POSS) as building blocks, were successfully deposited on various substrates, including cotton fabric. Water-soluble OctaAmmonium POSS ((+)POSS) and OctaTMA POSS ((-)POSS) were used as cationic and anionic components for thin film deposition from water. Aminopropyl silsesquioxane oligomer (AP) was also used as an alternative cationic species. The thickness of the AP/(-)POSS and (+)POSS/(-)POSS film is shown to increase linearly with bilayers deposited. Thermogravimetric analysis (TGA), vertical flame testing (VFT), microscale combustion calorimetry (MCC) and pill testing were performed on cotton fabric coated with 5–20 bilayers of a given recipe. All coated fabrics showed improved preservation (*i.e.*, greater residue following heating to 600 °C) and resistance to degradation from direct flame. With less than 8 wt % added to the total fabric weight, more than 12 wt % char remained following MCC for the 20 bilayers (+)POSS/(-)POSS coated cotton. Furthermore, afterglow time was reduced and the fabric weave structure and shape of the individual fibers were highly preserved following VFT. It is expected that this environmentally-friendly coating could be used to impart flame retardant behavior to a variety of fabrics, for protective clothing and soft furnishings, and other complex substrates like foam.

Introduction

The number of fire-related fatalities and amount of property damage has significantly declined worldwide in recent decades as legislation has forced a variety of polymeric materials to be rendered flame retardant (FR),[1,2] but as new fire scenarios occur, the need for new flame retardants continues. As of 1998, flame retardants were second only to plasticizers in terms of quantity added to plastics.[3] Brominated compounds continue to be the most commonly used flame retardants, but environmental concerns regarding brominated FR additives[4,5] have led to significant research into the use of other flame retardant chemistries and approaches, including polymer nanocomposites prepared from more environmentally benign nanoparticles like clays[6–8] and carbon nanotubes.[9,10] These polymer nanocomposites typically exhibit reduced mass loss and heat release rate, along with anti-dripping behavior, all of which is believed to be due to the formation of a barrier surface layer in the case of clay[7] and a gel-like network in the case of nanotubes.[11] Despite this improved thermal behavior, adding these particles is known to increase viscosity and modulus of the final polymeric material, making industrial processing difficult.[12] These adverse side effects of viscosity make their use in protection of fabrics prohibitive, and create a vitally important need for an alternative technology, such as a thin film coating.

Over the past two decades, layer-by-layer (LbL) assembly has been studied extensively as a simple and versatile method to develop multifunctional thin films.[13–16] The process typically involves alternately dipping substrates into aqueous mixtures of positively- and negatively-charged polymers and/or particles. Electrostatic attraction causes the charged substances to adsorb onto the surface one nano layer at a time, often creating a multilayer film less than one micron thick. The process is continued until the desired number of bilayers (BL) is reached. Some films exploit other forces such as covalent[17,18] or hydrogen bonds[19,20] instead of, or in addition to, electrostatic attraction. Spray coating[21] and spin coating[22,23] have been successfully used as alternatives to dipping the substrates. Film properties can be controlled by adjusting the deposition mixture conditions such as pH,[24,25] ionic strength,[26] and molecular weight[26,27] of the species, or by altering the temperature.[28,29] LbL films have been studied for applications that include sensing,[30,32] antimicrobial surfaces,[33] drug delivery and biomedical applications,[34–36] battery electrolytes,[37,38] superhydrophobic surfaces[39,40] and oxygen barrier layers.[41] It was also shown that coating cotton fabrics (one of the most important, but highly flammable, natural textiles[42]) with clay using LbL assembly, significantly preserved the weave structure after burning (and reduced heat release rate) by merely adding 1 to 4 wt % of the total fabric weight.[43,44] Additionally, this coating did not affect the physical and mechanical properties of the fabric. This flame retardant

Department of Mechanical Engineering, Polymer NanoComposites Laboratory, Texas A&M University, College Station, TX, 77843-3123, USA. E-mail: jgrunlan@tamu.edu; Fax: +1 979 862 3989; Tel: +1 979 845 3027

behavior created by thin coatings of layered silicates motivated the present study of silsesquioxane-based coatings.

Polyhedral oligomeric silsesquioxane (POSS) is a well-defined cluster with an inorganic core (Si_8O_{12}) surrounded by eight organic groups, which can reinforce polymer chain segments and control chain motions by maximizing the surface area and interaction with polymers in composites.[45,46] Additionally, POSS does not suffer from the increased processing viscosity typically associated with using other inorganic fillers.[47,48] This ease of uniformly dispersing POSS, using simple blending uniformly into polymers without further modification, has caused it to be investigated as a filler for polymer reinforcement and thermal property enhancement.[50,51] During burning in air, the organic groups on POSS cages can undergo homolytic Si–C bond cleavage ($\sim$ 300–350 °C), resulting in the fusion of the POSS cages and the formation of a thermally- and oxidatively-stable silicon-oxycarbide "blackglass" surface ("Si–O–C ceramified char") created from the initial $(RSiO_{1.5})_n$ composition.[52] The formation of this thin layer provides a physical char barrier against combustion, preventing the diffusion of oxygen into the underlying material (and also limiting heat transfer).[53] This is a very similar mechanism to that found in composites containing layered silicates.[54] Several POSS-containing polymer composites have been studied and they all showed improved combustion properties and greater char yields relative to unfilled polymers.[50,55,56] When polymers are in the form of fibers, flame retardants are conventionally applied during polymerization, or by spinning, and coating. Polypropylene (PP)-POSS multifilament yarn was made *via* a melt spinning process and knitted into fabrics, which showed that POSS could improve the thermal stability of PP by increasing the time to ignition (TTI).[57] A polyurethane (PU)-POSS system was coated onto polyester and cotton fabrics, with a thickness of 36 μm, and both showed reduced heat release rate (HRR) and longer TTI.[58]

In this work, two types of POSS, with positively-charged amino side chains and with negatively-charged oxide ions, were incorporated into LbL assemblies to provide flame resistance to cotton fabric. Others have explored the layer-by-layer growth of similiar types of POSS, but only a single type was paired with either polymers[59,60] or colloidal nanoparticles.[61,62] OctaAmmonium POSS® (denoted as (+)POSS) and OctaTMA POSS® (denoted as (-)POSS) were used to build thin films composed entirely of POSS nanocages. Another $(RSiO_{1.5})_n$ chemical, aminopropyl silsesquioxane oligomer (AP), was also used to assemble films with (-)POSS. The thickness and the mass composition of the two different films were characterized before applying them to cotton fabric to evaluate their thermal stabilities. Vertical flame testing, microscale combustion calorimetry, and a methenamine pill test were performed to evaluate the fire behavior of coated cotton. The best recipe is 20 BL of AP (pH 10)/(-)POSS (pH 10), which reduces the total heat release by 23%, and peak heat release rate (pHRR) by 20%, relative to uncoated cotton fabric. The coated fabrics were imaged with scanning electron microscopy (SEM) before and after flame testing. After flame testing, the residues are shown to maintain fiber shape and fabric weave structure. Fourier transform infrared spectroscopy (FTIR) was used to confirm the presence of POSS on the fibers. This work demonstrates that effective flame retardant coatings can be deposited on fabrics using layer-by-layer assembly of Si-containing molecules exclusively. With growing concern over toxicity of brominated flame retardants, this Si-based coating provides an environmentally-friendly alternative.

Experimental section

Chemical reagents and substrates

Aminopropyl silsesquioxane oligomer (AP, 23 wt % in water, Gelest, Inc. Morrisville, PA), octa(3-ammoniumpropyl) octasilsesquioxane octachloride (OctaAmmonium POSS®, (+)POSS) and octakis(tetramethylammonium) pentacyclo-[9.5.1.1^{3,9}.1^{5,15}.1^{7,13}] octasiloxane 1,3,5,7,9,11,13,15-octakis-(cyloxide)hydrate (OctaTMA POSS®, (-)POSS) (both from Hybrid Plastics®, Hattiesburg, MS), NaOH and HCl (both from Aldrich, Milwaukee, WI) were obtained commercially and used without further purification (see structure in Fig. 1). All solutions were prepared using 18.2 MΩ deionized water from a Direct-QTM 5 Ultrapure Water System (Millipore, Billerica, MA). Silicon wafers (University Wafer, South Boston, MA) were used as deposition substrates for ellipsometry and atomic force microscopy (AFM). Prior to deposition, silicon wafers were cleaned by immersion into "piranha" solutions (3 : 1 H_2SO_4/H_2O_2; dangerous if contacted with organics) for 1 h, followed by rinsing with deionized water. Polished Ti/Au crystals with a resonance frequency of 5 MHz (Maxtek, Inc. Cypress, CA) were used for quartz crystal microbalance (QCM) characterization. Desized, scoured and bleached plain-woven cotton fabric was supplied by the United States Department of Agriculture (USDA) Southern Regional Research Center (SRRC, New Orleans, LA). The fabric was a balanced weave with approximately 80 threads per inch in both the warp and fill directions, with a weight of 119 g m^{-2}. The control fabric referred to in this paper was treated by laundering through a cold water cycle, with no detergent, in a standard commercial high-efficiency clothes washer and dried for approximately 30 min in a commercial electric clothes dryer (Whirlpool Corporation, Benton Harbor, MI). The wet processing of the control fabric was intended to eliminate the variation derived from any changes in physical construction of the fabric due to the wet processing of the fabric during the LbL deposition, and the laundered fabric was then used as the uncoated fabric (*i.e.* control) in all tests.

Layer-by-layer deposition

1 wt % AP pH 10, 10 mM (+)POSS pH 7.5, and 10 mM (-)POSS pH 10 were prepared as the deposition solutions. All films were assembled on a given substrate using the procedure shown in Fig. 1. Each substrate was dipped into the ionic deposition solutions, alternating between the AP or (+)POSS (cationic) and (-)POSS (anionic), with each cycle corresponding to one bilayer (BL). The first dip into each mixture was five minutes, beginning with the cationic solution. Subsequent dips were one minute each. Every dip was followed by rinsing with deionized water and drying with a stream of filtered air for 30 s each. In the case of the fabrics, the drying step involved wringing the water out instead of air-drying. After achieving the desired number of BL, the coated wafers were dried with filtered air, whereas the fabrics were dried in a 70 °C oven for 2 h.

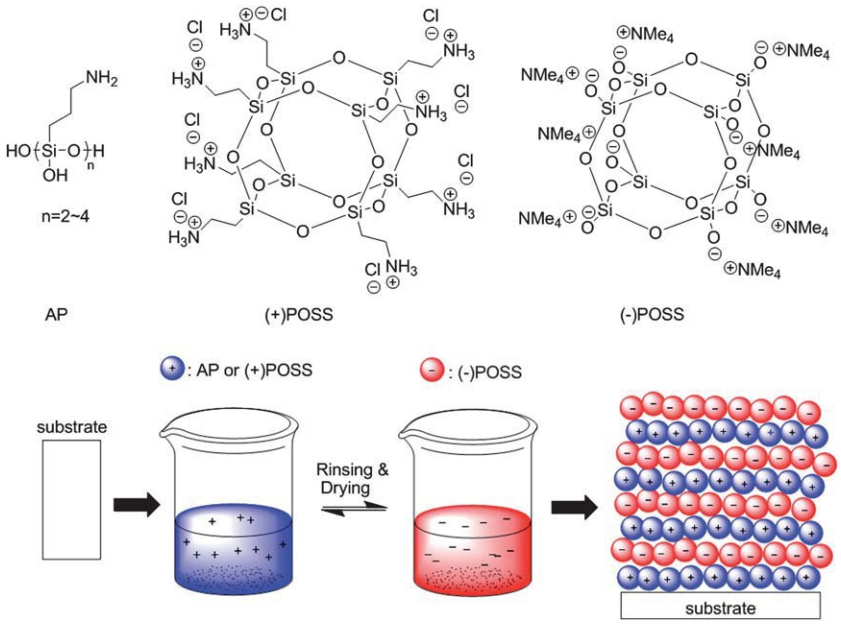

Fig. 1 Chemical structures of deposition materials[49] and schematic of the LbL deposition process used to prepare Si-based assemblies. Steps 1–4 are repeated until the desired number of bilayers is deposited.

Film growth characterization

Film thickness was measured on a silicon wafer using a PhE-101 Discrete Wavelength Ellipsometer (Microphotonics, Allentown, PA). The HeNe laser (632.8 nm) was set at an incidence angle of 65°. A Maxtek Research Quartz Crystal Microbalance from Infinicon (East Syracuse, NY), with a frequency range of 3.8–6 MHz, was used in conjunction with 5 MHz quartz crystals to measure the weight per deposited layer. Surface structures were imaged with a Nanosurf EasyScan 2 Atomic Force Microscope (Nanoscience Instruments, Inc., Phoenix, AZ). AFM images were gathered in tapping mode with a XYNCHR cantilever tip. Water contact angle measurements were done using a CAM 200 Optical Contact Angle Meter (KSV Instruments Ltd., Helsinki, Finland).

Thermal stability, flammability, combustibility, and ignition testing of fabrics

All dried fabrics were stored in desiccator prior to testing and all tests were conducted in triplicate to obtain the reported averages. The thermal stability of uncoated and coated fabrics was measured with a Q50 Thermogravimetric Analyzer (TA Instruments, New Castle, DE). Each sample was approximately 10 mg and was tested in both an air and nitrogen atmosphere, from room temperature to 600 °C, with a heating rate of 20 °C min^{-1}. Vertical flame testing was performed on 3 × 12 inch (7.62 × 30.48 cm) sections of uncoated and coated fabrics according to ASTM D6413. An Automatic Vertical Flammability Cabinet, model VC-2 (Govmark, Farmingdale, NY), was used to conduct this testing. Microscale combustibility experiments were conducted with a Govmark MCC-1 Microscale Combustion Calorimeter, according to ASTM D7309. The sample size was around 15 mg and samples were tested with a 1 °C s^{-1} heating rate under nitrogen from 200 to 600 °C. The pyrolysis volatiles released from the thermal degradation of the sample are pushed into a 900 °C combustion furnace where they are mixed with oxygen. The amount of oxygen consumed during that combustion process determines the heat released for the material at that temperature.[63] The timed methenamine burning tablet (Vesta Pharmaceutical Inc, Indianapolis, IN), used to simulate a small scale ignition test, was burned for 130 s under controlled conditions. This test is used to evaluate the response of textile floor covering materials to heat and flame. Specimens pass this test if the charred area is less than one inch (2.54 cm) in diameter.[64] The fabric size used for this test in this study is 4 × 6 inch (10.16 × 15.24 cm).

Analysis of fabric

Surface images of control and coated fabric, as well as afterburn residues (after direct exposure to flame), were acquired with a Quanta 600 field-emission scanning electron microscope (FE-SEM, FEI Company, Hillsboro, OR). Energy-dispersive X-ray (EDX) analysis was conducted with an Oxford system microanalyzer attached to the FE-SEM. An Alpha FT-IR (Bruker Optics Inc., Billerica, MA), with platinum ATR module, was used to characterize the coated fabrics and afterburn residues.

Results and discussion

Growth and structure of Si-based assemblies

1 wt % AP in deionized water has an unadjusted pH of 10.7. In order to have more protonated amine groups (*i.e.*, higher charge density) the solution was adjusted to pH 10 by adding 1 M HCl. For POSS solutions, in order to have the same amount of POSS molecules in both solutions, and also keep them similar to the concentration of the AP solution, 10 mM (+)POSS and (-)POSS solutions were prepared. Growth of these POSS-POSS

assemblies was evaluated at several pH values. The unadjusted pH of (+) and (-)POSS are 3.2 and 11.6, respectively, but films did not grow under these conditions. By adjusting the pH of (+)POSS to 7.5 and (-)POSS to 10, a film grew linearly as a function of the number of bilayers deposited. The diameter of the POSS cage is ~ 6 Å, so one bilayer of POSS may be expected to be around 1.4 nm. This corresponds with the thickness measured for the 30 BL POSS-only film shown in Fig. 2, which is 41.4 nm. The AP solution was adjusted to pH 10 to match (-)POSS. The growth of AP and (-)POSS was also examined as a function of BL deposited and this film also grew linearly, with a 30 BL film achieving a thickness of 89 nm.

Films were weighed during deposition using a QCM. When measured after each deposition step (Fig. 3), linear mass growth of the two films was revealed, just like the ellipsometric thickness trend (Fig. 2). A 30 BL AP/(-)POSS film has a mass of 5.77 μg cm^{-2}, while it is 2.58 μg cm^{-2} for a (+)POSS/(-)POSS film. These differences are due to both film thickness and density. The density of the films is mass per unit area divided by thickness. The density of the AP-film is 0.65 g cm^{-3} and the (+)POSS-film is 0.62 g cm^{-3}. AP is 46 wt % in AP/(-)POSS film and (+)POSS is 44 wt % in (+)POSS/(-)POSS film. An AP/(-)POSS film is thicker and heavier than a (+)POSS/(-)POSS film due to the AP molecules depositing more efficiently in each dipping cycle than (+)POSS. AP molecules are smaller (one quarter the molecular weight) and have less charge than (+)POSS. Hydrogen bonding among amino and hydroxyl groups on neighboring AP molecules likely form efficiently packed, stable AP aggregates, preventing them from being rinsed away between deposition steps.

Tapping mode AFM was used to characterize the surfaces of 30 BL AP/(-)POSS and (+)POSS/(-)POSS films. Fig. 4(a) and (b) show height and phase images of the AP-film, while Fig. 4(c) and (d) are height and phase images of the (+)POSS-film. A granular surface can be seen in both films, and this clustering/aggregation of POSS species has been observed by others.[65,66] It is interesting to note that the diameter of the clusters in the AP-film are larger than those in the (+)POSS-film, which may be further evidence of more AP molecules depositing on the film surface during each deposition step, resulting in more aggregation. The root-mean-square (rms) area roughness (using a 20 μm square area) for the AP-film is 9.3 nm, while it is 3.6 nm for the (+)POSS-film. In terms of roughness as a percentage of film thickness, the AP-film, which is 10.5%, is slightly rougher than the (+)POSS-film at 8.7%. This roughness likely contributes to the relatively high contact angle for the AP-film (91°) compared to the smoother (+)POSS-film (56.2°). Both of these films are more hydrophobic than the bare silicon wafer, which has a contact angle of 38.8°.

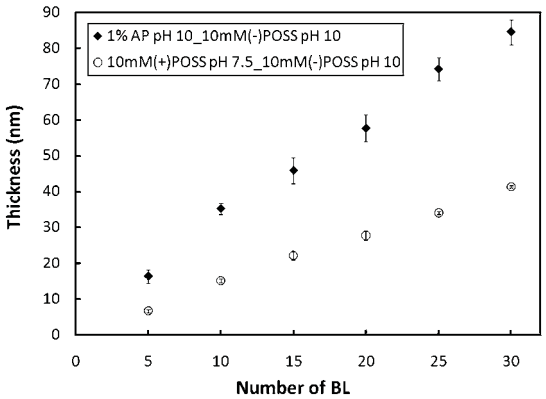

Fig. 2 Film thickness as a function of the number of bilayers deposited. Films were assembled from aqueous solutions with 1 wt % AP at pH 10 or 10 mM (+)POSS at pH 7.5, paired with 10 mM (-)POSS at pH 10.

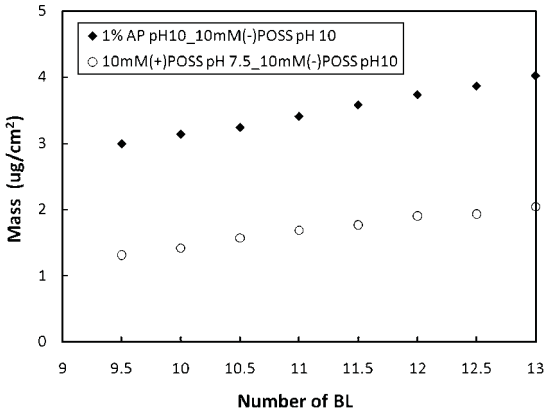

Fig. 3 Accumulated film mass as a function of deposited layers for the two 10 mM (-)POSS (pH 10)-based films.

Thermal properties of coated fabric

The AP/(-)POSS and (+)POSS/(-)POSS coatings characterized in the previous section were applied to cotton fabric. The as-received fabric is pure cellulosic fibers (starches, waxes and proteins were removed from the raw cotton fabric). Hydroxyl groups on cellulose have an isoelectric point of pH 2.5–3, which means that during the coating process, as long as the pH values of the dipping solutions are higher than 3, the zeta potential of the cellulose is negative (*i.e.*, it carries negative surface charge).[67] The coating process is similar to the process of coating a flat substrate, except for the drying step. In this case, liquid was wrung out of the fabric after every dipping and rinsing step. After coating, the fabrics were dried in an oven at 70 °C for two hours,

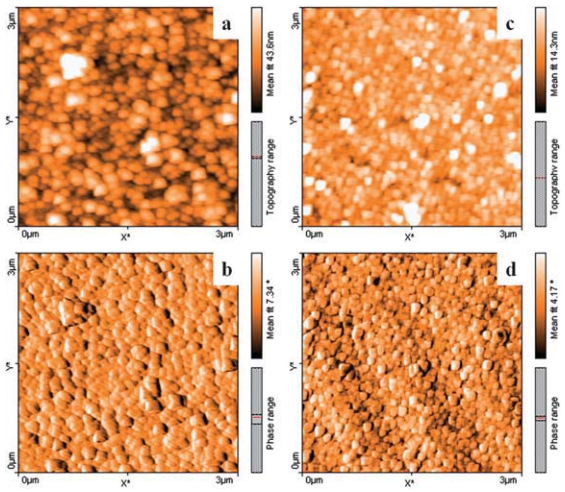

Fig. 4 AFM height (a) and phase (b) surface images of a 30 BL AP/(-)POSS film. Height (c) and phase (d) images of a 30 BL (+)POSS/(-)POSS film are also shown.

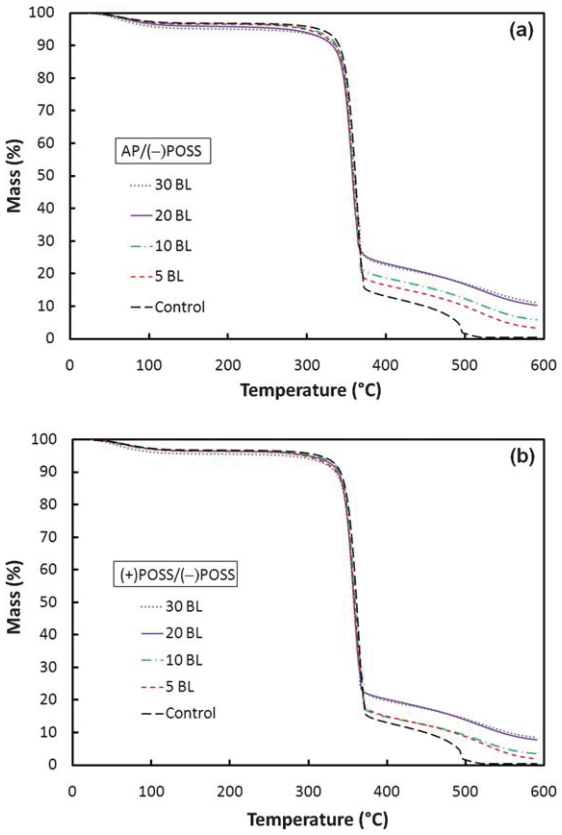

Fig. 5 Weight loss as a function of temperature for cotton fabrics coated with 5, 10, 20 and 30 bilayers of AP/(-)POSS (a) and (+)POSS/(-)POSS (b). Control refers to the uncoated cotton fabric.

and the coating weight was measured after the fabrics cooled to room temperature. The thermal properties of 5, 10, 20, and 30 BL-coated fabrics were examined by TGA, under both air and nitrogen atmospheres, with a heating rate of 20 °C min^{-1}. The mass % of the residue is plotted as a function of temperature in Fig. 5. Fig. 5(a) and (b) show AP-fabrics and (+)POSS-fabrics under air atmosphere, respectively. The uncoated control fabric begins to degrade around 350 °C and full degradation is reached near 500 °C. All coated fabrics have degradation curves similar to the control, but they show higher mass at 380 °C, and this mass gradually decreases all the way to 600 °C. This is in contrast to the control, which has a second abrupt mass drop before 500 °C that results in complete loss of residue.

The final residues of each coated fabric at 600 °C are directly related to the coating weight added. Residues increase with the number of bilayers added. In Table 1, the weight add-on is the percentage added by the coating to the original fabric weight. For both coating systems, the weight gain increased as the coating BL numbers increased, but not linearly, probably due to the complex geometry of the fabric surface, which does not allow more coating layered on fibers when the space between fibers are filled. The temperatures at 50% mass for all the fabrics are very close to one another, under both air and nitrogen. From Table 1 and Fig. 5, 20 and 30 BL of AP- and (+)POSS-coated fabrics have very similar residue weight left at 500 and 600 °C under both atmospheres, suggesting that the effective thickness limit on the fabric was reached. Thickness is believed to be somewhat limited by the tight spacing between individual cotton fibers that results in reduced deposition and some flaking off of the coating due to inter-fiber rubbing. Moreover, the 5 and 10 BL (+)POSS-coated fabrics have very similar curves on the plot and similar coating weight gain as well, suggesting that the first 10 BL were not very stable (*i.e.*, did not adhere to the fabrics very well) because of the small size of the molecules, which means relative few charged groups per molecule. It is not surprising that all the final residues are less than the coating wt %, because both AP and (+) POSS have organic side chains that easily volatilize at high temperatures. Both pure chemicals were run under the same TGA conditions in air, and AP had 59 wt % left and (+)POSS had 50 wt % left at 600 °C.

Fabrics coated with 5, 10 and 20 BL (30 BL not shown due to the limitations described above) of the AP and (+)POSS-based assemblies were subjected to vertical flame testing (ASTM D6413). Times to ignition for the control and all coated fabrics are very similar, within 0.5 s of one another, which is within error. After-flame time for all coated fabrics is 1 to 3 s longer than control. All burning processes were video-recorded and the images shown were captured from the videos at the same time. Differences of flame size can be distinguished, between the control and two different coated fabrics, as shown in Fig. 6. Six seconds after ignition, the size of the flame for the two 10 BL AP- and (+)POSS-coated fabrics is clearly smaller (in both

Table 1 Thermogravimetric analysis of control and eight different coated fabrics

		air			N_2		
Coating systems	add-on (%)	temperature at 50% mass	500 °C residue (%)	Final residue (%)	temperature at 50% mass	500 °C residue (%)	Final residue (%)
control	0	361.35	1.71	0.54	371.88	7.67	2.74
AP/(-)POSS							
5 BL	3.87	357.66	10.05	3.29	369.18	10.67	8.76
10 BL	7.48	358.05	12.67	6.01	370.16	12.77	8.86
20 BL	13.83	357.17	16.57	10.22	372.45	17.71	15.24
30 BL	14.2	359.66	16.84	10.91	371.15	18.54	15.08
(+)POSS/(-)POSS							
5 BL	4.63	359.22	8.36	1.88	369.64	9.7	6.91
10 BL	5.5	359.23	9.32	3.49	367.31	10.66	7.38
20 BL	7.42	357.32	14.02	7.89	368.38	14.74	11.59
30 BL	10.05	358.39	14.11	8.11	368.63	15.91	12.18

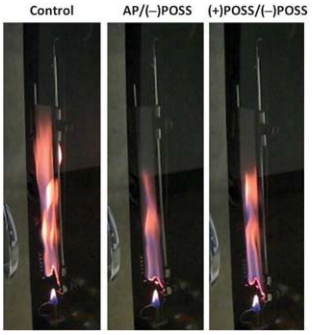

Fig. 6 Images of vertical flame testing of the uncoated and coated cotton fabrics 6 s after ignition. The coated fabrics are 10 BL of a given recipe.

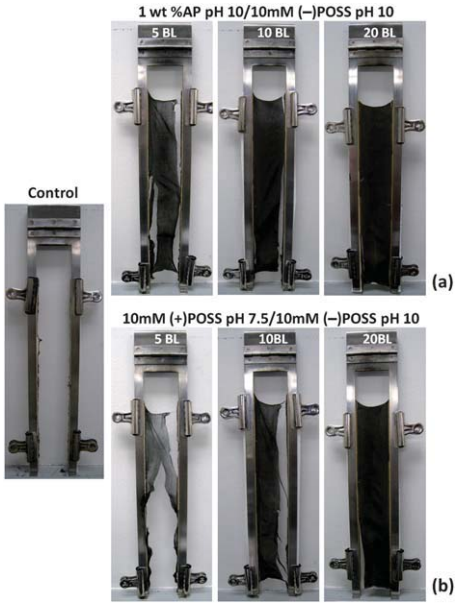

Fig. 7 Images of control, 5, 10, and 20 BL-coated cotton fabrics following the vertical flame test. Residues of fabrics coated with AP/(-)POSS (a), and (+)POSS/(-)POSS (b), are shown.

vertical and horizontal directions), and less bright, than the flame on the control fabric. In addition, more glow was observed on the control fabric after the flame was removed. The afterglow times for 8 different coated fabrics were 8 to 9 s less than the uncoated fabric, which was 10 s. In other words, once the flame on the control fabric died out, there was still glow along the edges of the residue. In the case of the coated fabrics, the glow disappeared in less than 2 s once the flame disappeared. Horizontal burn testing (ASTM D5132, not shown) revealed similar flame speed with or without a coating, although coated fabrics again displayed a diminished flame size. After burning, there was practically no char left from the control fabric, but all coated fabrics left significant residue, as shown in Fig. 7(a) and (b). In general, more bilayers on a fabric left more residue and char was darker after flame testing. Char weight was found to increase as the number of bilayers increased from 5 to 20.

Another small scale tool for assessing flammability is the microscale combustion calorimeter. The MCC simulates the burning process by using anaerobic pyrolysis, and a subsequent reaction of the volatile pyrolysis products with oxygen, under high temperatures to simulate surface gasification and flaming combustion.[63] Key parameters obtained from the MCC test include char yield (obtained by measuring the sample mass before and after pyrolysis), peak heat release rate peak (pkHRR is the recorded peak maximum of heat release rate during each experiment), pkHRR temperature (the temperature at which the pkHRR was measured), and total heat release. MCC data for the fabric samples are summarized in Table 2. Char from all coated fabrics is higher than that from uncoated fabric, with char yield increasing with more bilayers on the fabric. Greater char yield was accompanied by the lower total HR and pkHRR. The maximum reduction in total HR (23%) and HRR peak (20%), as compared to the control, are observed for the fabric coated with 20 BL of AP/(-)POSS. From the (+)POSS/(-)POSS coated fabrics, the best performance is also the 20 BL-coated fabric, which shows a 17% reduction in total HR and 11% in reduction in pkHRR.

In an effort to better observe the ignition characteristics of these coated fabrics, a pill test was performed. This test, which is much less severe than the vertical flame test, subjects textiles to a small source of glow, similar to a lighted cigarette.[68] The pill was placed in the center of the fabric and burned for 130 s. Two different 10 BL coated fabrics were tested, along with the control. The control fabric caught fire after the fabric started charring and was burned completely by the end of the test, as shown in Fig. 8(a). In contrast, the coated fabrics (Fig. 8(b) and (c)) did not catch fire, but only smoldered and charred around the tablet. The charred area gradually increased during the process but once the pill stopped burning and charring also stopped. The size of the char for AP-coated fabric was 7 × 20 mm and it was 7 × 53 mm for (+)POSS-coated fabric.

Characterization of burned fabric

Fabrics coated with 5, 10 and 20 BL of AP/(-)POSS and (+)POSS/(-)POSS were imaged by SEM prior to burning. Images of 30 BL-coated fabrics were omitted due to the similar coating weight and thermal behavior compared to fabric coated with 20 BL. The amount of AP/(-)POSS coating can be distinguished (top row in Fig. 9), where 5 BL-coated fibers are covered with a thin layer of the coating and some particulate-like aggregates.

More aggregates can be seen on 10 BL-coated fibers and a very thick layer of coating is on top of each fiber surface with 20 BL. At 20 BL, aggregates can even be seen in between the fibers, which helps explain the similar behavior for 30 BL-coated fabrics, because the spaces between fibers are filled with the coatings, (akin to reaching saturation). The weave structures of fabrics after burning were also examined (bottom row of Fig. 9). The 10 nm thickness and 3.8 wt % of coating from 5 BL AP/(-)POSS were enough to preserve the weave structure of fabric, although significant fiber shrinkage is observed. For 10 and 20 BL, the degree of shrinkage decreased with increasing bilayers.

The 20 BL residues in particular appear to have preserved the three-dimensional structure of the fabric weave. Unlike the 10 BL residue, where despite preserving the weave, they are flatter. In the case of (+)POSS/(-)POSS coated fabrics (top row images of Fig. 10), the coating amount also increased with increasing bilayers, but compared to the AP-coated fibers in Fig. 9, the amount of (+)POSS/(-)POSS coating appears to be much less.

Table 2 Microscale combustion calorimetry results for various coated fabrics

	Char yield (%)	pkHRR (W g^{-1})	pkHRR temperature (°C)	Total HR (kJ g^{-1})
control	4.98 ± 0.03	285 ± 2	380.67 ± 0.58	12.83 ± 0.06
AP/(-)POSS				
5 BL	7.47 ± 0.11	296 ± 4	373.33 ± 0.58	12.07 ± 0.06
10 BL	9.87 ± 0.19	274.33 ± 10.41	374.67 ± 1.15	11.67 ± 0.12
20 BL	14.13 ± 0.25	227.33 ± 5.86	377 ± 2	9.9 ± 0.2
(+)POSS/(-)POSS				
5 BL	6.02 ± 0.08	268 ± 18	374.33 ± 2.31	11.53 ± 0.15
10 BL	6.95 ± 0.06	292.33 ± 8.08	372 ± 1	12.33 ± 0.06
20 BL	12.23 ± 0.05	253.33 ± 6.11	376.67 ± 1.53	10.6 ± 0.1

Fig. 8 Pill test images of post-burn control fabric (a), 10 BL AP/(-)POSS coated fabric (b), and 10 BL of (+)POSS/(-)POSS coated fabric (c).

This reduced level of coating resulted in looser weave structures after burning (bottom row of Fig. 10) compared to the AP-coated residues coated with the same number of bilayers.

During vertical flame testing, the spot on the coated fabrics that first caught fire and started the burning process had a glow that persisted for several seconds. With the exception of this spot, the flame and glow stopped immediately once the triangular main flame passed through. The flame moved upward continuously and left residue the size of the original sample. At the end of the burning, the residue is dark brown, except for the initial ignition spot, which is white. This white-colored char is seen in all coated fabrics, except 5 BL of (+)POSS/(-)POSS, and its area increases with the number of bilayers deposited. In contrast, the control fabric has no char at all. As the main flame passed through, the control was completely consumed, leaving persistent glow at the edges of the sample holder. Fig. 11(a) is the 20 BL AP/(-)POSS coated fabric after burning. The white spot was imaged under SEM, which shows some broken fibers that are hollow (Fig. 11(b)). Under higher magnification (Fig. 11(c)), the hollow tube is clearly visible, with a diameter of 10 μm that is similar to the diameter of individual fibers before burning. The Si-based oligomers and nanocages may have gone through bond breaking and re-formed a network-like structure to create a continuous ceramic tube that was hollowed out after the cellulosic core (*i.e.*, cotton fiber) was completely burned out. The surface of the hollow tube was subjected to EDX analysis (Fig. 11(d)) and showed very strong Si and O peaks, suggesting an amorphous silica structure,[59] with some trace carbon left from the cellulose.

The FTIR spectrum of uncoated cotton fabric exhibits an O–H stretching absorption around 3300 cm^{-1}. As the number of deposited bilayers increases, these absorbance peaks (of uncoated fabric) decrease due to shielding from the AP/(-)POSS,

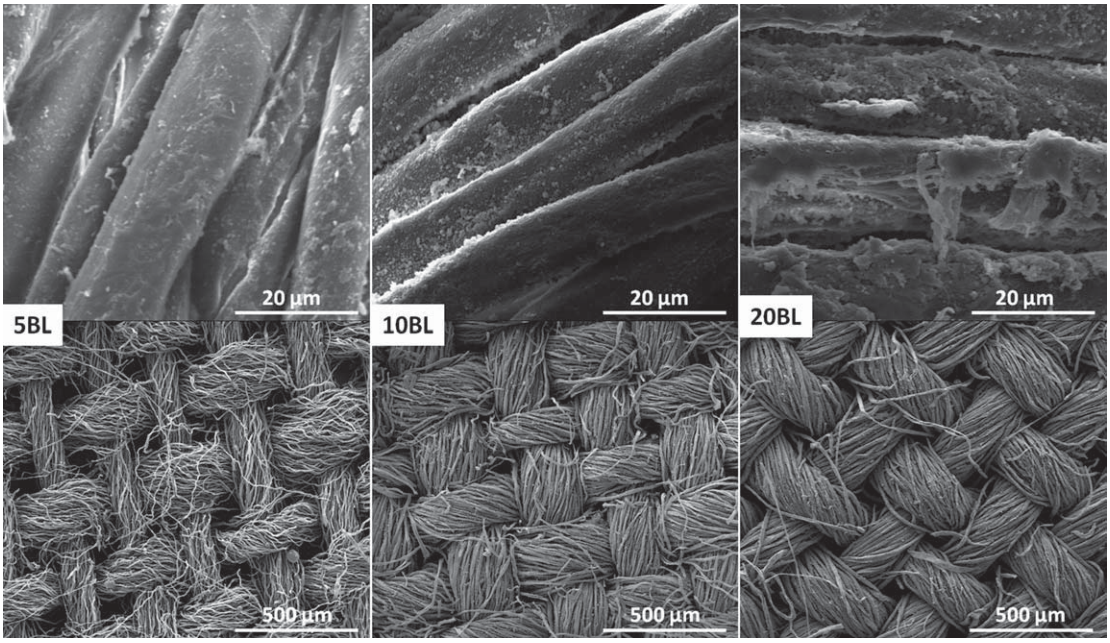

Fig. 9 SEM images of 5, 10 and 20 BL of AP/(-)POSS coated fabrics. The top row images are coated fabrics before flame testing, while bottom row images show the weave structure of residues after burning the coated fabrics in the vertical flame test.

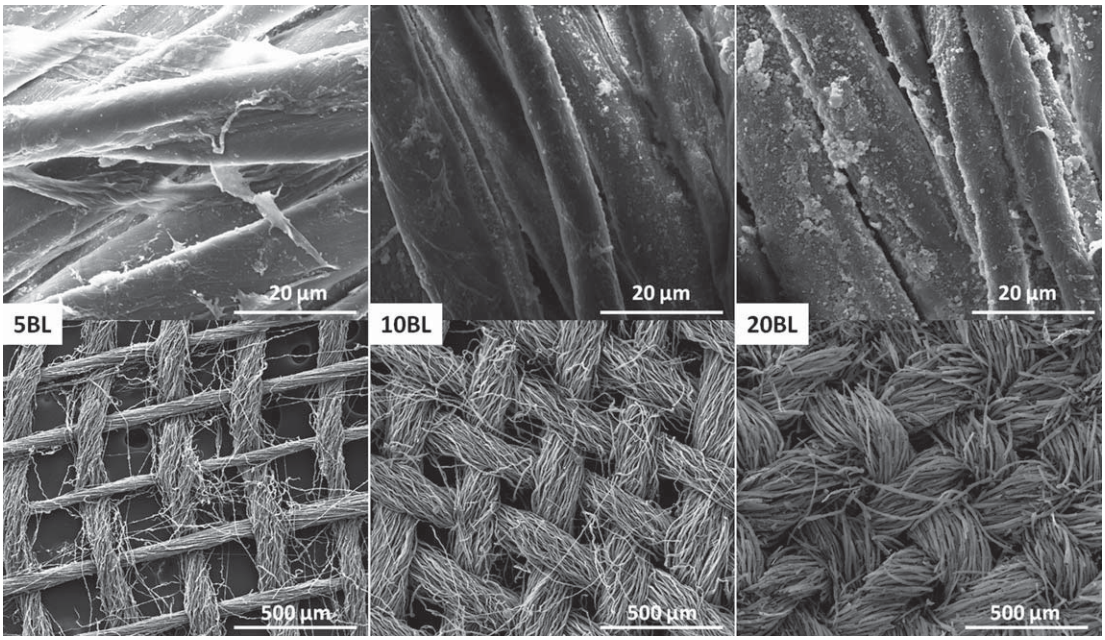

Fig. 10 SEM images of 5, 10 and 20 BL of (+)POSS/(-)POSS pH 10 coated fabrics. The top row images are coated fabrics before flame testing, while bottom row images show the weave structure of residues after burning the coated fabrics in the vertical flame test.

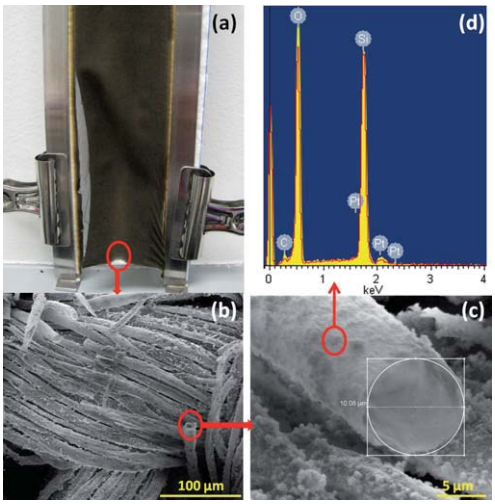

Fig. 11 Residue of 20 BL of AP/(-)POSS coated fabric after vertical flame testing (a), SEM image of the white char (b), higher magnification SEM image of the hollow siliceous fiber tube (c), and EDX analysis of the hollow tube (d).

as shown in Fig. 12(a). No major absorbance peaks from the coating are observed in the spectrum except a small peak at 795 cm^{-1} that is from Si–C bonds on AP, but it is only seen at higher bilayers. The same situation is observed for (+)POSS/(-)POSS coated fabrics. After vertical flame testing, the residues of coated fabrics were also examined with FTIR. Characteristic absorbance peaks of cellulose (from 2500 to 3500 cm^{-1}) are missing from the char of the coated fabrics, as shown in Fig. 12(b). Very strong absorption is seen at 1050 cm^{-1}, from Si–O–Si asymmetric stretching. This peak is believed to be caused by stretching from the network structure rather than stretching from the POSS cages, which occurs at $\sim$ 1110 cm^{-1}.[55] This would explain the

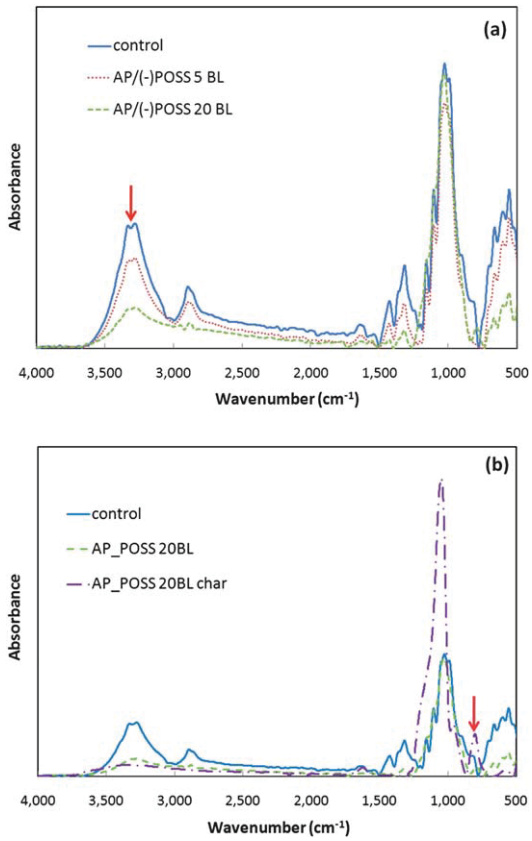

Fig. 12 FTIR spectrum of control and AP/(-)POSS coated fabrics, at 5 and 20 BL (a). Spectrum comparison of AP/(-)POSS 30 BL coated fabric, char and white char.

ceramic tube shown in Fig. 11(c). Another unique absorption peak on the char is at 805 cm^{-1}, which is from Si–O–Si symmetric stretching. Similar spectra are found with (+)POSS/(-)POSS coated fabrics and chars.

Conclusions

Layer-by-layer assemblies of Si-oligomer and charged POSS were successfully grown on flat substrates and on cotton fabric, growing linearly as a function of bilayers deposited. AP/(-)POSS assemblies deposit thicker and heavier layers than (+)POSS/(-)POSS assemblies, possibly due to hydrogen bonding among the AP oligomer's side chains. Fabrics coated with these two recipes showed greatly reduced afterglow times during vertical burn testing and the weave structures on their residues are highly preserved compared to the uncoated fabric. The fabric coated with 20 BL of 1 wt % AP pH 10/10 mM (-)POSS pH 10 exhibits the greatest reduction in total heat release (23% compared to the control) and peak of heat release rate (20%), as measured by microscale combustion calorimetry. Additionally, coated fabrics show good performance in the methenamine pill test, which mimics a small scale fire (*e.g.*, from a smoldering cigarette). If furnishing textiles are flame retardant, there is a reduced chance for a large-scale fire to progress from a small-scale fire source, which ultimately saves lives and property. In addition to their flame retardant behavior, these Si-based thin films may be useful for other applications, such as low dielectric constant for lowering signal delay, due to their nanoporous structure.[65,66] It is also possible that inorganic micro-tubes could be produced using this technique of burning out the polymeric core, which may be easier than using the more traditional etching of an inorganic template.[69–72]

Acknowledgements

The authors would like to acknowledge the Building and Fire Research Laboratory (BFRL) at the National Institute of Standards and Technology (NIST) for financial support of this work, and the USDA Southern Regional Research Center (SRRC) for providing cotton fabric. The FE-SEM acquisition was supported in part by the National Science Foundation under Grant No. DBI-0116835. The authors also thank Y.–H. Yang for assistance with SEM imaging.

Notes and references

1 S. V. Levchik, in *Flame Retardant Polymer Nanocomposites*, ed. A. B. Morgan and C. A. Wilkie, Wiley & Sons, Hoboken, NJ, 2007.
2 G. L. Nelson and C. A. Wilkie, in *Fire and Polymer IV: Materials and Concepts for Hazard Prevention*, ed. C. A. Wilkie and G. L. Nelson, ACS Symposium Series 922; American Chemical Society, Washington, DC, 2006.
3 J. Q. Wang and W. K. Chow, *J. Appl. Polym. Sci.*, 2005, **97**, 366–376.
4 C. A. de Wit, *Chemosphere*, 2002, **46**, 583–624.
5 I. Watanabe and S. Sakai, *Environ. Int.*, 2003, **29**, 665–682.
6 G. Guo, C. B. Park, Y. H. Lee, Y. S. Kim and M. Sain, *Polym. Eng. Sci.*, 2007, **47**, 330–336.
7 J. W. Gilman, R. H. Harris, J. R. Shields, T. Kashiwagi and A. B. Morgan, *Polym. Adv. Technol.*, 2006, **17**, 263–271.
8 J. Zhu, P. Start, K. A. Mauritz and C. A. Wilkie, *Polym. Degrad. Stab.*, 2002, **77**, 253–258.
9 S. Peeterbroeck, F. Laoutid, B. Swoboda, J. M. Lopez-Cuesta, N. Moreau, J. B. Nagy, M. Alexandre and P. Dubois, *Macromol. Rapid Commun.*, 2007, **28**, 260–264.
10 B. Schartel, P. Potschke, U. Knoll and M. Abdel-Goad, *Eur. Polym. J.*, 2005, **41**, 1061–1070.
11 T. Kashiwagi, F. M. Du, J. F. Douglas, K. I. Winey, R. H. Harris and J. R. Shields, *Nat. Mater.*, 2005, **4**, 928–933.
12 S. S. Ray and M. Okamoto, *Prog. Polym. Sci.*, 2003, **28**, 1539–1641.
13 K. Ariga, J. P. Hill and Q. Ji, *Phys. Chem. Chem. Phys.*, 2007, **9**, 2319–2340.
14 G. Decher, in *Multilayer Thin Films: Sequential Assembly of Nanocomposite Materials*, ed. G. Decher and J. B. Schlenoff, Wiley-VCH, Weinheim, Germany, 2003.
15 P. Bertrand, A. Jonas, A. Laschewsky and R. Legras, *Macromol. Rapid Commun.*, 2000, **21**, 319–348.
16 P. Podsiadlo, B. S. Shim and N. A. Kotov, *Coord. Chem. Rev.*, 2009, **253**, 2835–2851.
17 J. Q. Sun, T. Wu, F. Liu, Z. Q. Wang, X. Zhang and J. C. Shen, *Langmuir*, 2000, **16**, 4620–4624.
18 D. E. Bergbreiter and B. S. Chance, *Macromolecules*, 2007, **40**, 5337–5343.
19 D. E. Bergbreiter, G. L. Tao, J. G. Franchina and L. Sussman, *Macromolecules*, 2001, **34**, 3018–3023.
20 F. Lv, Z. H. Peng, L. L. Zhang, L. S. Yao, Y. Liu and L. Xuan, *Liq. Cryst.*, 2009, **36**, 43–51.
21 K. C. Krogman, J. L. Lowery, N. S. Zacharia, G. C. Rutledge and P. T. Hammond, *Nat. Mater.*, 2009, **8**, 512–518.
22 Y. M. Lee, D. K. Park, W. S. Choe, S. M. Cho, G. Y. Han, J. Park and P. J. Yoo, *J. Nanosci. Nanotechnol.*, 2009, **9**, 7467–7472.
23 S. L. Song and N. F. Hu, *J. Phys. Chem. B*, 2010, **114**, 3648–3654.
24 S. S. Shiratori and M. F. Rubner, *Macromolecules*, 2000, **33**, 4213–4219.
25 P. Bieker and M. Schonhoff, *Macromolecules*, 2010, **43**, 5052–5059.
26 J. E. Wong, A. M. Diez-Pascual and W. Richtering, *Macromolecules*, 2009, **42**, 1229–1238.
27 Z. J. Sui, D. Salloum and J. B. Schlenoff, *Langmuir*, 2003, **19**, 2491–2495.
28 H. L. Tan, M. J. McMurdo, G. Q. Pan and P. G. Van Patten, *Langmuir*, 2003, **19**, 9311–9314.
29 L. Chang, X. Kong, F. Wang, L. Wang and J. Shen, *Thin Solid Films*, 2008, **516**, 2125–2129.
30 H. H. Yu, T. Cao, L. D. Zhou, E. D. Gu, D. S. Yu and D. S. Jiang, *Sens. Actuators, B*, 2006, **119**, 512–515.
31 P. H. B. Aoki, D. Volpati, A. Riul, W. Caetano and C. J. L. Constantino, *Langmuir*, 2009, **25**, 2331–2338.
32 H. F. Cui, Y. H. Cui, Y. L. Sun, K. Zhang and W. D. Zhang, *Nanotechnology*, 2010, **21**, 5601–5608.
33 C. M. Dvoracek, G. Sukhonosova, M. J. Benedik and J. C. Grunlan, *Langmuir*, 2009, **25**, 10322–10328.
34 Q. He, Y. Cui and J. B. Li, *Chem. Soc. Rev.*, 2009, **38**, 2292–2303.
35 T. Boudou, T. Crouzier, K. F. Ren, G. Blin and C. Picart, *Adv. Mater.*, 2010, **22**, 441–467.
36 H. W. Chien, T. Y. Chang and W. B. Tsai, *Biomaterials*, 2009, **30**, 2209–2218.
37 M. Yang, S. F. Lu, J. L. Lu, S. P. Jiang and Y. Xiang, *Chem. Commun.*, 2010, **46**, 1434–1436.
38 F. Wang, M. Alazemi, I. Dutta, R. H. Blunk and A.A.P., *J. Power Sources*, 2010, **195**, 7054–7060.
39 Y. Zhao, Y. W. Tang, X. G. Wang and T. Lin, *Appl. Surf. Sci.*, 2010, **256**, 6736–6742.
40 J. N. Ashcraft, A. A. Argun and P. T. Hammond, *J. Mater. Chem.*, 2010, **20**, 6250–6257.
41 W. S. Jang, I. Rawson and J. C. Grunlan, *Thin Solid Films*, 2008, **516**, 4819–4825.
42 P. J. Wakelyn, N. R. Bertoniere, A. D. French and D. Thibodeaux, ed., *Cotton Fiber Chemistry and Technology*, CRC Press (Taylor and Francis Group), Boca Raton, FL, 2007.
43 Y.-C. Li, J. Schulz and J. C. Grunlan, *ACS Appl. Mater. Interfaces*, 2009, **1**, 2338–2347.
44 Y.-C. Li, J. Schulz, S. Mannen, C. Delhom, B. Condon, S. Chang, M. Zammarano and J. C. Grunlan, *ACS Nano*, 2010, **4**, 3325–3337.
45 P. G. Harrison, *J. Organomet. Chem.*, 1997, **542**, 141–183.
46 S. W. Kuo, H. C. Lin, W. J. Huang, C. F. Huang and F. C. Chang, *J. Polym. Sci., Part B: Polym. Phys.*, 2006, **44**, 673–686.

47 R. A. Mantz, P. F. Jones, K. P. Chaffee, J. D. Lichtenhan, J. W. Gilman, I. M. K. Ismail and M. J. Burmeister, *Chem. Mater.*, 1996, **8**, 1250–1259.
48 J. J. Schwab and J. D. Lichtenhan, *Appl. Organomet. Chem.*, 1998, **12**, 707–713.
49 Hybrid Plastics (http://www.hybridplastics.com).
50 L. Liu, Y. Hu, L. Song, S. Nazare, S. Q. He and R. Hull, *J. Mater. Sci.*, 2007, **42**, 4325–4333.
51 R. Misra, B. X. Fu and S. E. Morgan, *J. Polym. Sci., Part B: Polym. Phys.*, 2007, **45**, 2441–2455.
52 S. K. Gupta, J. J. Schwab, A. Lee, B. X. Fu and B. S. Hsiao, in SAMPE pub., ed. B. M. Rasmussen, L. A. Pilato and H. S. Lkliger, Long Beach, CA, 2002, p. 1571.
53 G. H. Hsiue, Y. L. Liu and H. H. Liao, *J. Polym. Sci., Part A: Polym. Chem.*, 2001, **39**, 986–996.
54 M. Zanetti, T. Kashiwagi, L. Falqui and G. Camino, *Chem. Mater.*, 2002, **14**, 881–887.
55 A. Fina, D. Tabuani and G. Camino, *Eur. Polym. J.*, 2010, **46**, 14–23.
56 Y. Feng, Y. Jia, S. Y. Guang and H. Y. Xu, *J. Appl. Polym. Sci.*, 2010, **115**, 2212–2220.
57 S. Bourbigot, M. Le Bras, X. Flambard, M. Rochery, E. Devaux and J. D. Lichtenhan, in *Fire retardancy of polymers: New applications of mineral fillers*, ed. M. Le Bras, B. S. and C. A. Wilkie, Royal Society of Chemistry, Cambridge, UK, 2005.
58 E. Devaux, M. Rochery and S. Bourbigot, *Fire Mater.*, 2002, **26**, 149–154.
59 T. Cassagneau and F. Caruso, *J. Am. Chem. Soc.*, 2002, **124**, 8172–8180.
60 X. M. Wang, H. M. Ding, Y. K. Shan and M. Y. He, *Chin. Chem. Lett.*, 2004, **15**, 1227–1229.
61 J. B. Carroll, B. L. Frankamp, S. Srivastava and V. M. Rotello, *J. Mater. Chem.*, 2004, **14**, 690–694.
62 J. A. Lee, K. C. Krogman, M. L. Ma, R. M. Hill, P. T. Hammond and G. C. Rutledge, *Adv. Mater.*, 2009, **21**, 1252–1256.
63 B. Schartel, K. H. Pawlowski and R. E. Lyon, *Thermochim. Acta*, 2007, **462**, 1–14.
64 ASTM International. Designation D 2859-06.
65 G. J. Wu and Z. H. Su, *Chem. Mater.*, 2006, **18**, 3726–3732.
66 Y. L. Liu, C. S. Liu, W. H. Chen, S. Y. Chen, K. S. Wang and M. J. Hwu, *J. Nanosci. Nanotechnol.*, 2009, **9**, 1839–1843.
67 D. H. Marsh, D. J. Riley, D. York and A. Graydon, *Particuology*, 2009, **7**, 121–128.
68 E. J. Blanchard, E. E. Graves and P. A. Salame, *J. Fire Sci.*, 2000, **18**, 151–164.
69 Z. L. Xiao, C. Y. Han, U. Welp, H. H. Wang, W. K. Kwok, G. A. Willing, J. M. Hiller, R. E. Cook, D. J. Miller and G. W. Crabtree, *Nano Lett.*, 2002, **2**, 1293–1297.
70 C. D. Bae, S. Y. Kim, B. Y. Ahn, J. Y. Kim, M. M. Sung and H. J. Shin, *J. Mater. Chem.*, 2008, **18**, 1362–1367.
71 Y. F. Mei, D. J. Thurmer, C. Deneke, S. Kiravittaya, Y. F. Chen, A. Dadgar, F. Bertram, B. Bastek, A. Krost, J. Christen, T. Reindl, M. Stoffel, E. Coric and O. G. Schmidt, *ACS Nano*, 2009, **3**, 1663–1668.
72 M. H. Park, M. G. Kim, J. Joo, K. Kim, J. Kim, S. Ahn, Y. Cui and J. Cho, *Nano Lett.*, 2009, **9**, 3844–3847.

ADVANCED MATERIALS
www.advmat.de

Materials Views
www.MaterialsViews.com

Intumescent All-Polymer Multilayer Nanocoating Capable of Extinguishing Flame on Fabric

*Yu-Chin Li, Sarah Mannen, Alexander B. Morgan, SeChin Chang, You-Hao Yang, Brian Condon, and Jaime C. Grunlan**

According to the National Fire Protection Association (NFPA), there were an estimated 1.3 million fires in the United States in 2009, which resulted in 3010 civilian deaths (one every 175 minutes), 17 050 injuries (one every 31 minutes),[1] and direct property loss estimated at $12.5 billion. There were more than 40 000 deaths worldwide from fire in 2006 and it cost every country an average of 1% of their gross domestic product in property loss, medical services for burn victims, etc.[2] Fire-related issues continue to drive the development of materials that can reduce fire risk to save lives and protect property, but any flame retardants used to reduce that fire risk have to meet various safety standards to reduce the deleterious effect on the environment or human health. Textiles in particular require effective anti-flammable performance combined with minimal enviornmental impact because they are often washed and flame retardant additives can leach out of the fabric and into the environment.[3,4] There are numerous strategies used to make textile fibers flame retardant: surface treatment, fire-retardant additives or co-monomers in synthetic fibers, nanocomposite technology, heat-resistant and inherently fire-retardant fibers, and fiber blending.[5] More recently, layer-by-layer (LbL) assembly has been used as a surface treatment to impart flame resistance to cotton fabric by coating each individual fiber with a clay-polymer nanobrick wall.[6]

LbL is a simple and versatile method to incorporate various polymers, colloids, or molecules into a thin film that is typically no thicker than 1 μm.[7–9] These nanocoatings are deposited by alternately exposing a substrate to positively and negatively charged ingredients that are adsorbed as nanolayers, most often through electrostatic attraction. Numerous functionalities have been imparted to substrates with LbL nanocoatings,[10–13] but flame-retardant behavior (from clay/polyelectrolyte nanocomposite thin films on cotton fabric),[6,14] was only recently demonstrated for the first time. Anti-flammability of cotton fabric was shown to be enhanced through thermogravimetric analysis (TGA) and microscale cone calorimetry (MCC). Silica nanoparticles,[15,16] and polyhedral oligomeric silsesquioxanes (POSS),[17] were also used to create the flame-retardant nanocoatings via LbL assembly. Although these coatings showed improved flame spread behavior (i.e., slower burning across the surface) for cotton fabric, they did not really prevent the fabric from burning. More specifically, they did not completely inhibit ignition, nor did they allow the fabric to become self-extinguishing due to their passive nature. These nanoparticle-based coatings showed a flame-retardant effect primarily through creating a physical barrier on the textile fibers. This barrier was formed by a silicate species via the same mechanism found in bulk polymer-clay nanocomposites.[18,19]

An effective alternative to fire protection by inorganic barrier formation is fire protection through intumescence (i.e., carbon foam formation from high heat or fire). Intumescent coatings suppress flammability through a condensed-phase mechanism, by interrupting the polymer combustion process of fuel generation and heat feedback from burning polymer decomposition products (i.e., an active rather than passive mechanism).[20,21] This process results from a combination of charring the decomposing polymer, which involves converting it to graphitic or glassy carbon rather than fuel, and foaming this carbonaceous residue at the surface of the burning polymer. The resulting cellular charred layer, whose density decreases as a function of temperature, protects the underlying material from the action of the heat flux or the flame.[22] This charred layer then acts as a physical barrier that slows down heat and mass transfer between the gas and condensed phases.

Traditional intumescent flame retardants contain four components: a source of carbon (or carbon donor), a source of acid (or acid donor), a source of gas (or blowing agent), and a binder to keep all the components suspended in a liquid dispersion and form a solid film on a surface.[23] Intumescent coatings have traditionally been used to protect macroscopic objects such as steel beams, using millimeters thick layers that expand to centimeters during foaming.[24] Here, the first ever intumescent nanocoating is demonstrated using LbL assembly of poly(sodium phosphate) (PSP), which acts as the acid source and is negatively charged in water, and poly(allylamine) (PAAm), which is used as the blowing agent and is positively charged in water (see chemical structures in **Figure 1**). As PAAm degrades, low-molecular-weight compounds are released that act as blowing

Dr. Y.-C. Li, S. Mannen, Y.-H. Yang, Prof. J. C. Grunlan
Department of Mechanical Engineering
Materials Science and Engineering Program
Texas A&M University
3123 TAMU, College Station, TX 77843, USA
E-mail: jgrunlan@tamu.edu
Dr. A. B. Morgan
Multiscale Composites and Polymers Division
University of Dayton Research Institute
300 College Park, Dayton, OH 45469, USA
Dr. S. Chang, Dr. B. Condon
Southern Regional Research Center (SRRC)
United States Department of Agriculture (USDA)
1100 Robert E. Lee Blvd. New Orleans, LA 70124, USA

DOI: 10.1002/adma.201101871

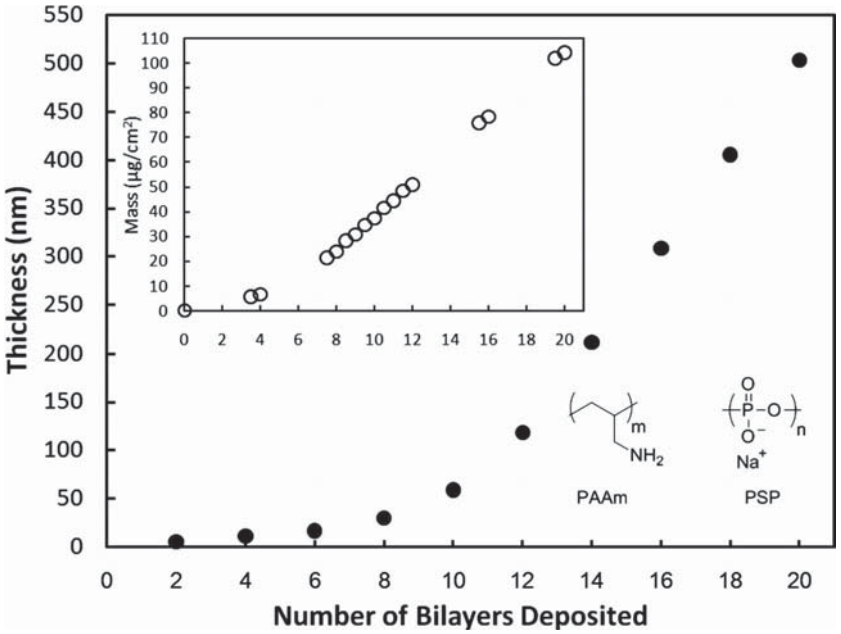

Figure 1. Film thickness as a function of the number of bilayers deposited. The first layer deposited was BPEI, followed by alternating layers of PSP and PAAm, i.e., PSP/PAAm bilayers deposited. The inset shows accumulated film mass as a function of deposited layers. Half bilayers represent PAAm deposition.

gas (e.g., NH_3 is released and reacts with O_2 to form N_2 and H_2O). Thin films made with these two chemicals are conformally deposited onto cotton fabric, eliminating the need for a binder. Cellulose itself functions as the carbon source,[25] creating a complete intumescent system. This study demonstrates the ability to completely prevent ignition of cotton using an environmentally friendly, water-based technology.

PSP/PAAm bilayers were deposited on silicon wafers, using branched polyethylenimine (BPEI) as a primer layer to improve adhesion, to measure growth of this system, as shown in Figure 1. The first 10 bilayers (BL) grow somewhat exponentially and are much thinner compared to the next 10 BL, which grow thicker and more linearly. A similar growth trend was also found with assemblies of PSP/poly (allylamine hydrochloride) (PAH).[26] The weight growth trend (inset of Figure 1) is similar to thickness growth, which grows more slowly for the first few bilayers and more linearly thereafter. From the linear (steady-state) mass growth, this film was found to be composed of 62.1 wt% PSP and 37.9 wt% PAAm, which is about equal molarity based upon the repeat unit of each polymer. A film density of 2.07 g cm^{-3} was also calculated from these thickness and weight measurements.

This intumescent PSP/PAAm system was next applied to cotton fabric (presoaked in pH 2 water to increase the positive surface charge), in varying numbers of bilayers. Presoaking eliminated the need to use the BPEI primer on cotton. With a 5 BL coating, the fabric maintained a similar hand (i.e., feel) as uncoated cotton, but there was some modest stiffening of the fabric as greater numbers of layers were deposited. All coated fabrics show a lower degradation temperature, as measured by thermogravimetric analysis, when compared to the control fabric. Decomposition occurred near 320 °C, 30 °C lower than the control, and this degradation also finished nearly 40 °C earlier, at around 340 °C. Even with an earlier onset of degradation, all coated fabrics exhibited much higher residual weight than the control beyond 400 °C (**Figure 2**a). The coating weight of the coated fabric increased as the bilayer number increased (coating weight is 1.6%, 6%, and 17.5% for 5, 10 and 20 BL coated fabric with respect to the original fabric, as shown in Table S1, Supporting Information). The final mass for coated fabric was 2% to 7% higher than the coating weight percent added to the fabric, suggesting the fabric itself was preserved to some extent, protected by the char formed from the early degradation or oxidation.

These same coated fabrics were subjected to vertical flame testing (VFT). The uncoated control fabric was completely consumed by direct flame, while coated fabric, even with only a 5 BL coating (coating weight 1.6% with respect to the fabric weight), has 19.3 wt% residue left and was preserved as a complete piece. Char weight was 11 times greater than the coating weight added on the fabric, meaning the cotton had been incorporated into the carbonized layers and the residue was not coming from the coating. With more bilayers, the char weight% increased after burning. 10 BL fabric burned similarly to the fabric coated with 5 BL, but the unburned area on the fabric increased, as shown in Figure 2b. With a 6 wt% (10 BL) coating on cotton, there was 41 wt% residue left after flame testing. As for the 20 BL-coated fabric, the flame extinguished right after ignition for two of three samples (Figure 2b shows more than 95 wt% fabric retained after burning), meaning the char is durable enough to prevent additional cotton decomposition and pyrolysis and starve the flame of fuel. In one trial out of three the flame extinguished, but smoldered through the fabric (still had some uncharred part) and had 59.2 wt% residue remaining. During all burnings, the flame color and size on the coated fabric was less bright and smaller than the flame on the control fabric. With increasing BL on coated fabric, the flame looked much less aggressive during burning, as shown in Figure 2c. After-flame time was 6 s less than the control and there was no afterglow for all coated fabric samples. The flame spreading speed, once the fabric ignited, was measured with a horizontal flame test (HFT). 5 BL-coated fabric exhibits a fast burning rate relative to the control (247.4 mm min^{-1} versus 203.7), while no burning rate can be measured for 10 and 20 BL-coated fabric. For these higher bilayers, there was only smolder progression that stopped before the scribed line for measurement (see Figure S1, Supporting Information). There was no char left from the control fabric after HFT, but the residues from all coated fabrics look similar to the residues from VFT.

In an effort to better understand the burn behavior of PSP/PAAm-coated fabric, afterburn residues were imaged with scanning electron microscopy (SEM), as shown in **Figure 3**. The weave structures of all coated fabrics were largely retained

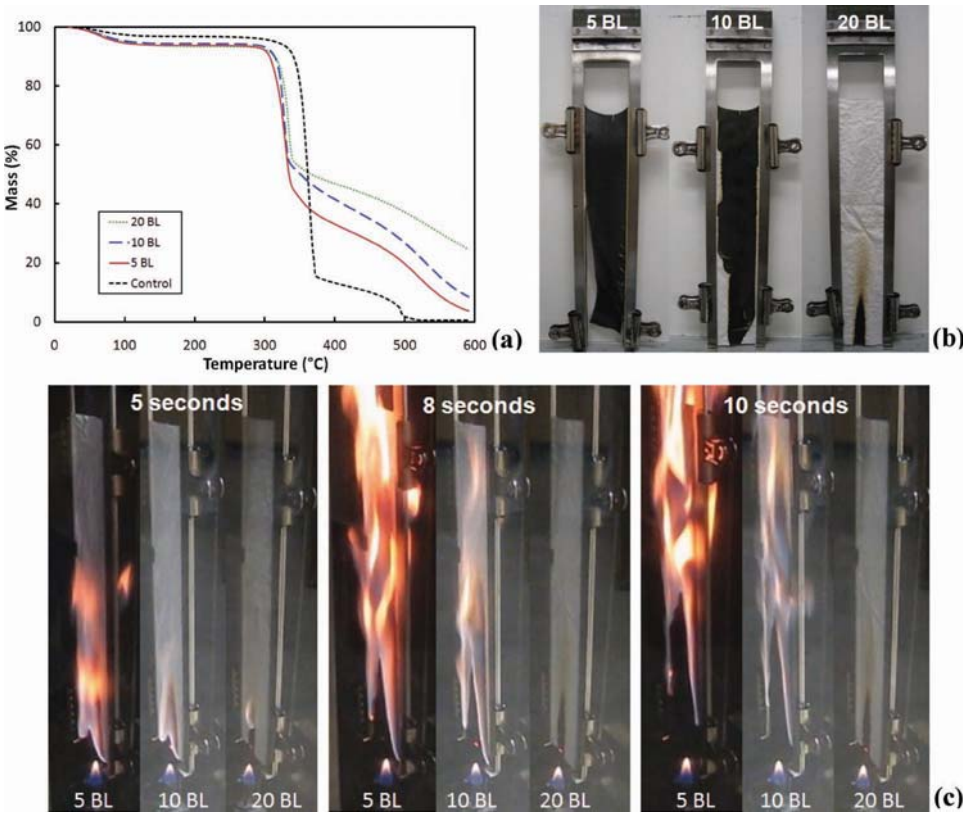

Figure 2. Weight loss as a function of temperature for fabric coated with varying numbers of PSP/PAAm bilayers (a). Post-burn images of three coated fabrics following vertical flame testing (b) and images during the flame testing recorded at 5, 8, and 10 s (c).

after burning. Additionally, these coatings did not alter the weave structure of the fabric prior to burning (i.e., the LbL nanocoating conformally coated each individual fiber) and no shrinkage of the cotton thread was observed after burning. At higher magnification, the coating on the fibers can be more clearly distinguished with regard to the number of bilayers and these images clearly show how conformal these nanocoatings are. The control fiber has a smooth surface and 5 BL-coated fabric looks very similar in terms of fiber structure and shape. When the BL number increases to 10, some fibers appear linked together and the gaps between fibers gradually disappear.

A closer look at the coated fabrics after burning reveals evidence of intumescent behavior. Fibers in the 5 BL fabric mantain their integrity after burning, with some fibers unwound. With a 10 BL nanocoating, fibers still have the same shape and size, very similiar to the fibers before burning. When the number of bilayers reached 20, the afterburn images looked different. The surface of the fibers looked very rough, and there were bubbles on top and in the gap between fibers, which is believed to be due to swelling and expansion of the nanocoating due to the intumescent effect. This image demonstrates the intumescent action of the thin coating that protects the fibers by forming a swollen layer, which prevents fabric from burning further, preserving weave structure and fiber integrity. It should be noted that most intumescent coatings typically have char bubbles/foam structure that can be easily seen with the naked eye due to macroscale carbon foam formation during burning, so at first glance one may be inclined to call the LbL effect one of strong char formation and not exactly intumescence. It seems likely that the bubbles observed here are indeed due to carbon bubbles being created by non-flammable gases, as occurs in macroscale intumescent formulations. Regardless of the foam size, the observed fire behavior does seem to suggest a carbon-based protective coating that slows (or stops) mass loss and flame spread, which is precisely how an intumescent coating works.

Control, 5, 10, and 20 BL of PSP/PAAm-coated fabrics were tested with the microscale cone calorimeter for assessing the heat release and flammability. There is a major reduction in total heat release (THR) and peak heat release rate (HRR) for coated fabric, as shown in **Table 1**. Comparing the uncoated control to the 5 BL fabric, the char yield increases from 9.6 to 23.8 wt%, with only 1.7% weight from the coating. The THR reduces to half of the value from control fabric as a result of the coating. Peak HRR also drops significantly, going from 253 down to 146 W g^{-1}. The peak HRR of coated fabric occurs at a lower temperature than that of the control, suggesting a decrease in thermal stability for the whole system, which was also observed in TGA testing. This decreased thermal stability is believed to be due to the low-temperature reactions that occur within the intumescent coating that keep heat release low. If the intumescent char does not activate quickly after heat exposure, the flame will consume the sample, so the lowered decomposition temperaure is likely necessary and not a defect of the system. With the 10 and 20 BL samples, both the peak HRR and the

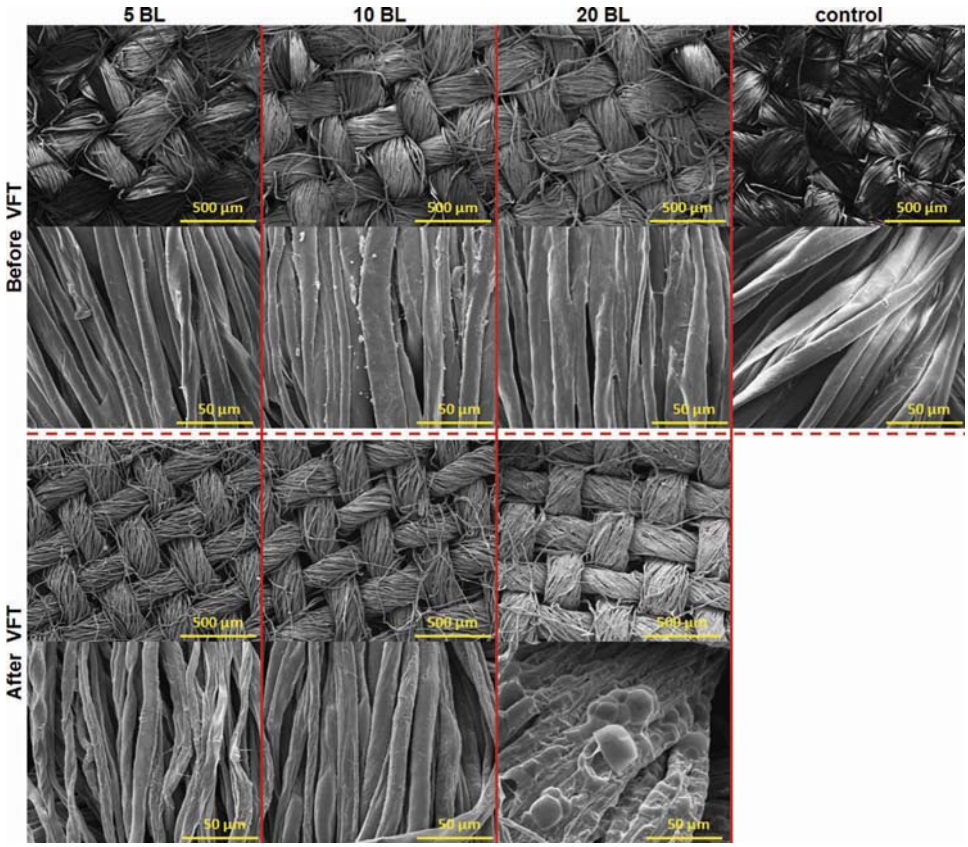

Figure 3. SEM images of control (uncoated) fabric and fabric coated with 5, 10, and 20 BL of PSP/PAAm before burning. After-burn SEM images of 5, 10, and 20 BL of PSP/PAAm-coated fabric are also shown.

THR decrease, but the 20 BL sample has a slightly higher value than the 10 BL. The 20 BL fabric also exhibits a relatively small secondary peak at an elevated temperature (shown as a second value for peak HRR and temperature at peak HRR in Table 1). It is believed that this second peak is additional char formation from the extra 10 BL of coating, which burns off as a small HRR event around 415 °C.

Control and coated fabrics were also tested with a cone calorimeter at a 35 kW m^{-2} heat flux. 5 BL-coated fabric yielded erratic fire behavior, with two samples igniting at different times and one sample not igniting at all. When the sample did not ignite, the smoke released increased (see Table S2, Supporting Information). This is an expected result because mass is still pyrolyzing off the surface of the sample, but since it does not burn (no flaming combustion) smoke is generated instead. None of the 10 BL samples ignited at all, even after 180 s of total exposure time. The effective antiflammable behavior, observed with flame testing, seems to cause the erratic heat release behavior, which could be just the baseline data (noise) and not actual measured heat release. While the 20 BL sample consistently ignited quickly, it also went out quickly and gave off low heat release. Due to the short burning duration, the final chars of 20 BL samples show very little black char damage (residue of all fabrics following the cone caloritmetry are shown in Figure S2). It appears that 10 BL is an optimal amount of fire protection coating for this fabric. Higher amounts of LbL coating actually increase the ignition and flammability behavior of the fabric, which is attributed to the coating itself acting as fuel.

It is clear that the use of intumescent nanocoatings greatly lowers the flammability of cotton fabric under a 35 kW m^{-2} heat flux. Based upon the observed fire behavior, it is believed that the intumescent effect is inhibiting sustained ignition at this heat flux, or greatly suppressing the amount of gas available for burning. Sometimes the coating is overwhelmed at this heat flux (i.e., sample ignites and burns) and in other cases the char sets up faster than the heat damage can occur and there is no ignition, or reduced heat release/increased smoke occurs. It is likely that the chars formed here are thermally stable enough that a heat flux of 35 kW m^{-2} cannot maintain ignition and a higher heat flux is needed to fully ignite these materials. Even with this erratic

Table 1. Microscale combustion calorimetry measurements of PSP/PAAm-coated fabric.

Sample	Char % [Yield]	HRR Peak(s) [W g^{-1}]	HRR Peak Temp [°C]	THR [kJ g^{-1}]
Control	9.59 ± 0.61	252.94 ± 8.18	399.68 ± 1.25	11.77 ± 0.23
5 BL	23.83 ± 1.96	145.67 ± 14.47	306 ± 2.65	5.77 ± 0.4
10 BL	31.43 ± 0.06	97.33 ± 7.09	302.67 ± 4.73	2.87 ± 0.12
20 BL	31.07 ± 0.38	92.33 ± 16.2, 16.67 ± 2.08	306.67 ± 4.73, 414.67 ± 1.15	3.8 ± 0.17

ignition behavior, when the samples ignite, the heat release is not very high, which is a desired result for an effective anti-flammable coating. These results demonstrate that this coating provides a powerful flame retardant effect and yields durable char structures that cannot easily burn through (or disintegrate upon burning).

In conclusion, LbL assemblies of PSP and PAAm were successfully deposited on various substrates, including cotton fabric. By applying these thin coatings on fabric, afterglow is eliminated and after-flame time is reduced in VFT. Flame was completely extinguished on fabric coated with 20 BL of PSP/PAAm. Post-burn chars were imaged with SEM and the weave structure, and fiber shape and structure, are shown to be well preserved. Especially on the 20 BL char, bubbles were formed on the fiber surfaces during burning, which is believed due to an intumescent effect. From microscale calorimetry data, the peak heat release rate and total heat release of fabric show a 43% and 51% reduction compared to the control fabric, with only 1.7 wt% coating added. This work demonstrates the first ever intumescent nanocoating prepared using LbL assembly. These all-polymer coatings provide an environmentally friendly alternative for protecting fabrics (no need for chemical treatments) such as cotton and lay the groundwork for rendering many other complex substrates (e.g., foam) flame-retardant without altering their processing and desirable mechanical behavior. The opportunity for further improvements is tremendous through the use of alternate polymers, nanoparticles, and/or smaller molecules that may enhance these effects.

Experimental Section

Chemicals and Substrates: PAAm (molecular weight, Mw = 15 000, 15 wt% in water; Polysciences, Inc., Warrington, PA), PSP (crystalline, +80 mesh, 96%, Aldrich, Milwaukee, WI), BPEI (Mw = 25 000, Aldrich), and sodium montmorrilonite clay (MMT) (cloisite Na^+, Southern Clay, Gonzales, TX) were used as received. 1 M HCl and 1 M NaOH (Aldrich) were used for adjusting the pH of the deposition solutions. Silicon wafers (University Wafer, South Boston, MA) and polished Ti/Au crystals with a resonance frequency of 5 MHz (Maxtek, Inc., Cypress, CA) were used for film characterization. Desized, scoured, and bleached plain-woven cotton fabric (with a weight of 119 g m^{-2}) was supplied by the United States Department of Agriculture (USDA) Southern Regional Research Center (SRRC, New Orleans, LA).

LbL Deposition and Film Growth Characterization: Separate 2 wt% PSP at pH 7 and 1 wt% PAAm at pH 7 were prepared with deionized water (18.2 MΩ) as separate deposition solutions. 1 wt% BPEI solution (at pH 10) was used to deposit a primer layer in the assembly, to create positive surface charge, and to improve adhesion to the substrates (silicon wafer and quartz crystal). All films were assembled on a given substrate, which was dipped into the ionic deposition solutions, alternating between the anionic PSP and cationic PAAm, with each cycle corresponding to one bilayer. The first dip into each mixture was for 5 min, beginning with the anionic solution. Subsequent dips were for 1 min each. Every dip was followed by rinsing with deionized water and drying with a stream of filtered air for 30 s each. For the fabric coating, in order to get higher positive surface charge,[27] the fabric was soaked in pH 2 deionized water for 5 min before deposition. Drying of fabric involved wringing the water out instead of air-drying. After achieving the desired number of bilayers, the coated wafers were dried with filtered air, whereas the fabrics were dried in an 80 °C oven for 1 h. Film thickness was measured on silicon wafers using an alpha-SE Ellipsometer (J. A. Woollam Co., Inc., Lincoln, NE). A Maxtek Research Quartz Crystal Microbalance (QCM) from Infinicon (East Syracuse, NY), with a frequency range of 3.8–6 MHz, was used to measure the weight per deposited layer. Surface images of coated fabrics, as well as of the chars from fabrics (after direct exposure to flame), were acquired with a Quanta 600 FE-SEM (FEI Company, Hillsboro, OR).

Thermal Stability, Flammability, and Combusitiblity of Fabric: All tests were conducted in triplicate to obtain the reported averages. The thermal stability of uncoated and coated fabrics was measured with a Q50 Thermogravimetric Analyzer (TA Instruments, New Castle, DE). Each sample was approximately 10 mg and was tested in an air atmosphere, from room temperature to 600 °C, with a heating rate of 20 °C min^{-1}. Vertical and horizontal flame testing was performed on 3 (and 4) in. × 12 in. sections of uncoated and coated fabrics according to ASTM D6413 and D5132, respectively. Automatic vertical and horizontal flammability cabinets (VC-2 and HC-2) (Govmark, Farmingdale, NY) were used to conduct these tests. Microscale combustibility experiments were conducted with a Govmark MCC-1 Microscale Combustion Calorimeter, according to ASTM D7309 method A. The sample size was 15 mg and samples were tested with a 1 °C s^{-1} heating rate under nitrogen, from 200 to 600 °C. Cone calorimeter experiments were conducted on a FTT Dual Cone Calorimeter at a 35 kW m^{-2} heat flux, with an exhaust flow of 24 L s^{-1}, using the standardized cone calorimeter procedure (ASTM E1354). All samples were mounted horizontally as per a modified cone calorimeter standard (ASTM E1740) and the sample size was 4 in. × 4 in. Specifically, samples were laid onto a foil wrapped ceramic (4 in.) square brick and then held down with a metal frame accroding to ASTM E1740.

Supporting Information

Supporting Information is available from the Wiley Online Library or from the author.

Acknowledgements

The authors would like to acknowledge the Building and Fire Research Laboratory (BFRL) at the National Institute of Standards and Technology (NIST) for financial support of this work. The FE-SEM acquisition was supported in part by the National Science Foundation under Grant No. DBI-0116835.

Received: May 19, 2011
Published online: July 29, 2011

[1] M. J. Karter, Jr., *NFPA J.* **2010**, *104*, 56
[2] International Association of Fire and Rescue Service website, http://www.ctif.org, (accessed March 2011).
[3] E. D. Weil, S. V. Levchik, *J. Fire Sci.* **2008**, *26*, 243.
[4] A. R. Horrocks, *Polym. Degrad. Stab.* **2011**, *96*, 377.
[5] B. K. Kandola, in *Fire Retardancy of Polymeric Materials*, (Eds: C. A. Wilkie, A. B. Morgan), Taylor and Francis Group CRC Press, Boca Raton **2010**, 725.
[6] Y. C. Li, J. Schulz, S. Mannen, C. Delhom, B. Condon, S. Chang, M. Zammarano, J. C. Grunlan, *ACS Nano* **2010**, *4*, 3325.
[7] G. Decher, in *Multilayer Thin Films: Sequential Assembly of Nanocomposite Materials*, (Eds: G. Decher, J. B. Schlenoff), Wiley-VCH, Weinheim, Germany **2003**.
[8] P. Bertrand, A. Jonas, A. Laschewsky, R. Legras, *Macromol. Rapid Commun.* **2000**, *21*, 319.
[9] K. Ariga, J. P. Hill, Q. Ji, *Phys. Chem. Chem. Phys.* **2007**, *9*, 2319.
[10] C. M. Dvoracek, G. Sukhonosova, M. J. Benedik, J. C. Grunlan, *Langmuir* **2009**, *25*, 10322.
[11] Y. T. Park, A. Y. Ham, J. C. Grunlan, *J. Mater. Chem.* **2011**, *21*, 363.

[12] M. A. Priolo, D. Gamboa, K. M. Holder, J. C. Grunlan, *Nano Lett.* **2010**, *10*, 4970.
[13] T. J. Dawidczyk, M. D. Walton, W. S. Jang, J. C. Grunlan, *Langmuir* **2008**, *24*, 8314.
[14] Y. C. Li, J. Schulz, J. C. Grunlan, *ACS Appl. Mater. Interfaces* **2009**, *1*, 2338.
[15] G. Laufer, F. Carosio, R. Martinez, G. Camino, J. C. Grunlan, *J. Colloid Interf. Sci.* **2011**, *356*, 69.
[16] F. Carosio, G. Laufer, J. Alongi, G. Camino, J. C. Grunlan, *Polym. Degrad. Stab.* **2011**, *96*, 745.
[17] Y. C. Li, S. Mannen, J. Schulz, J. C. Grunlan, *J. Mater. Chem.* **2011**, *21*, 3060.
[18] M. Zanetti, T. Kashiwagi, L. Falqui, G. Camino, *Chem. Mater.* **2002**, *14*, 881.
[19] H. L. Qin, S. M. Zhang, C. G. Zhao, G. J. Hu, M. S. Yang, *Polymer* **2005**, *46*, 8386.
[20] R. Delobel, M. Lebras, N. Ouassou, F. Alistiqsa, *J. Fire Sci.* **1990**, *8*, 85.
[21] S. Zhang, A. R. Horrocks, *J. Appl. Polym. Sci.* **2003**, *90*, 3165.
[22] S. Bourbigot, M. Lebras, R. Delobel, *J. Fire Sci.* **1995**, *13*, 3.
[23] B. K. Kandola, A. R. Horrocks, *Fire Mater.* **2000**, *24*, 265.
[24] M. Jimenez, S. Duquesne, S. Bourbigot, *Ind. Eng. Chem. Res.* **2006**, *45*, 7475.
[25] A. R. Horrocks, B. K. Kandola, P. J. Davies, S. Zhang, S. A. Padbury, *Polym. Degrad. Stab.* **2005**, *88*, 3.
[26] N. Cini, T. Tulun, G. Decher, V. Ball, *J. Am. Chem. Soc.* **2010**, *132*, 8264.
[27] D. H. Marsh, D. J. Riley, D. York, A. Graydon, *Particuology* **2009**, *7*, 121.